nutraceuticals

MDPI

Article

Alkali-Neutralization-Induced β-1,3-1,6-Glucan Nanoparticles Enhance the Aqueous Dispersibility, Stability, and Antioxidant Activity of Quercetin

Shoma Kannan [1], Nanako Doi [1], Toshio Suzuki [2] and Kazuya Koumoto [1,*]

[1] Department of Nanobiochemistry, Faculty of Frontiers of Innovative Research in Science and Technology (FIRST), Konan University, 7-1-20 Minatojima-minamimachi, Chuo-ku, Kobe 650-0047, Hyogo, Japan; m2561016@s.konan-u.ac.jp (S.K.); d.nanako723@gmail.com (N.D.)
[2] Department of Gastronomic Innovation, Faculty of Food and Nutrition Science, Tezukayama Gakuin University, 4-2-2, Harumidai, Minami-ku, Sakai 590-0113, Osaka, Japan; t-suzuki@tezuka-gu.ac.jp
* Correspondence: koumoto@konan-u.ac.jp; Tel.: +81-78-303-1465

Abstract

Quercetin is a nutraceutical flavonoid whose aqueous use is limited by poor solubility and chemical instability. Existing polysaccharide carriers may require chemical modification, crosslinkers, multicomponent formulations, or complex processing. Here, alkali-neutralization-induced β-1,3-1,6-glucan nanoparticles (r-glucan NPs), prepared from *Aureobasidium pullulans* K-1 glucan, were compared with β-cyclodextrin (β-CD), using native t-glucan as a composition-matched control. Spectroscopic analyses supported quercetin association with chiral, cavity-rich domains of r-glucan NPs. r-Glucan NPs showed higher quercetin loading than β-CD and increased apparent aqueous solubility/dispersibility to 1620 ± 15.3 μM, compared with 256 ± 0.52 μM for the native β-1,3-1,6-glucan control, 347 ± 16.4 μM for β-CD, and 7.11 ± 3.97 μM for free quercetin. The t-glucan control initially retained quercetin but showed limited aqueous dispersibility and formed a visible precipitate within 3 days in 1 vol% ethanol. Although carrier association reduced oxygen radical absorbance capacity (ORAC) activity on an equal-quercetin basis, r-glucan NPs yielded a maximum ORAC value of 11,600 ± 1200 μmol TE L^{-1}, compared with 815 ± 235 for β-CD and 368 ± 38.2 for free quercetin. r-Glucan NPs also improved apparent retention, photostability, stability at pH 6.8, and cellular antioxidant activity relative to free quercetin. These results support r-glucan NPs as food-compatible carriers for aqueous quercetin delivery.

Keywords: quercetin; renatured β-1,3-1,6-glucan nanoparticles; aqueous dispersibility; antioxidant activity; photostability; pH-dependent stability; Caco-2 cells; nutraceutical delivery

Academic Editor: Michael Netzel

Received: 31 May 2026
Revised: 29 July 2026
Accepted: 7 August 2026
Published: 14 August 2026

1. Introduction

Quercetin is a representative dietary flavonoid widely distributed in fruits, vegetables, and grains, and has attracted considerable interest as a functional food and nutraceutical ingredient because of its antioxidant, anti-inflammatory, and other health-promoting properties [1,2]. These biological activities make quercetin a promising candidate for use in beverages, supplements, and health-related formulations. However, its practical application in aqueous and oral formulations remains limited by its extremely low water solubility and poor stability under gastrointestinal conditions. The aqueous solubility of

quercetin has been reported to be approximately 0.01 mg mL^{-1} [3], which severely restricts its homogeneous dispersion in water-based products. In addition, quercetin is susceptible to degradation and/or chemical transformation under gastrointestinal conditions, resulting in low oral bioavailability, reportedly less than 2% [4]. Therefore, an effective delivery system that improves the aqueous dispersibility, stability, and functional availability of quercetin is required for its broader use as a nutraceutical ingredient.

Various formulation strategies have been investigated to improve the poor water compatibility of quercetin, including cyclodextrin-based inclusion complexes, emulsions, microemulsions, liposomes, and polymeric nanoparticles [5–9]. Among these systems, β-cyclodextrin (β-CD) is one of the most widely studied carriers because its hydrophobic cavity can partially accommodate hydrophobic guest molecules and improve their apparent aqueous solubility through host–guest complexation [10]. However, the capacity of native β-CD to solubilize quercetin is limited, and chemical modification of cyclodextrins is often required to further enhance complexation efficiency or formulation performance [3,11]. Although such modifications can improve binding affinity and aqueous solubility, they may also increase structural complexity and raise additional considerations for food and nutraceutical applications, where simple composition, safety, and regulatory acceptability are important. Emulsion-based systems can also improve quercetin dispersion [5,12], but their practical use may be constrained by formulation complexity, physical instability, and the need for surfactants or oil phases. Thus, there remains a need for food-compatible carrier materials that can maintain quercetin in aqueous media while preserving its functional activity.

Naturally derived polysaccharides have been investigated as carriers for quercetin because their chemical functionality and self-assembly or gel-forming properties can be used to improve the stability, delivery, and biological availability of poorly water-soluble quercetin [5,8,13–16]. For example, quercetin-loaded chitosan/alginate nanoparticles were reported to exhibit a favorable safety profile and enhanced antioxidant protection compared with free quercetin [14]. Quercetin-loaded chitosan nanoparticles prepared by ionic gelation with polyanionic crosslinkers also improved mucoadhesion, intestinal cell permeation, and cellular antioxidant activity [8]. In addition, starch-based nanoparticles have been used to encapsulate quercetin through noncovalent interactions, resulting in improved loading, protection, and prolonged bioactivity [15]. Porous starch/inulin microcapsules have likewise been shown to improve the thermal and photochemical stability of quercetin and provide sustained release [16]. These studies demonstrate the utility of polysaccharide-based carriers for improving quercetin protection and delivery. However, the reported systems rely on different formulation processes: chitosan-based nanoparticles generally require ionic crosslinking and multicomponent polymer matrices, starch nanoparticles are often prepared by nanoprecipitation, and starch/inulin systems are commonly formulated as microcapsules. Consequently, their properties can depend strongly on polymer composition, crosslinker identity, polymer ratio, and processing conditions. Moreover, these representative systems were primarily evaluated for protection, controlled release, or intestinal delivery and were not necessarily designed or evaluated for maintaining high concentrations of quercetin as a homogeneous aqueous dispersion. Therefore, there remains a need for a structurally simple, crosslinker-free, and food-compatible polysaccharide carrier that combines high aqueous dispersibility with effective quercetin retention and functional activity.

Among naturally derived polysaccharides, β-1,3-1,6-glucan is particularly attractive because of its biocompatibility, characteristic higher-order structure, and reported immunomodulatory activity [17,18]. However, native high-molecular-weight β-1,3-1,6-glucan generally exhibits limited aqueous dispersibility [18,19]. Previously reported glucan-based

carrier systems have often relied on top-down processing, in which bioactive compounds are loaded into or onto micron-scale glucan particles [20,21]. Such micron-scale systems remain particulate in water, and their loading and release behavior can depend strongly on the preparation method, limiting their suitability as homogeneous aqueous carriers for poorly water-soluble nutraceutical ingredients [20,21].

To address these limitations, we previously developed alkali-neutralization-induced, partially renatured β-1,3-1,6-glucan nanoparticles, hereafter referred to as r-glucan NPs, using a bottom-up self-assembly approach [19]. In this process, the native triple-helical structure of β-1,3-1,6-glucan is dissociated under alkaline conditions, followed by partial renaturation and nanoparticle formation during neutralization. This molecular reassembly generates hydrophobic cavity-like microenvironments capable of incorporating poorly water-soluble guest molecules. Importantly, r-glucan NPs are formed without chemical derivatization or crosslinkers. They have been shown to incorporate and solubilize poorly water-soluble bioactive molecules in neutral aqueous media [19] and to allow modulation of guest molecule release by changing the molecular weight of the constituent glucan chains [22].

We hypothesized that r-glucan NPs would provide multivalent, cavity-rich microenvironments capable of maintaining quercetin in aqueous media more effectively than β-CD while preserving its antioxidant functionality. To extend the applicability of the glucan nanoparticle platform beyond the previously studied curcumin system [22], quercetin was selected as a structurally and functionally distinct flavonol. Quercetin contains multiple phenolic hydroxyl groups and exhibits strong peroxyl-radical-scavenging activity, which is directly relevant to the oxygen radical absorbance capacity (ORAC) assay used in this study. At the same time, quercetin is susceptible to pH-dependent degradation and oxidative transformation [23–25]. Quercetin therefore provides a stringent model for evaluating whether the glucan nanoparticle platform can improve the aqueous dispersibility and chemical stability of a redox-active flavonoid without substantially compromising its antioxidant functionality. β-CD was used as a representative benchmark carrier. To isolate the effect of alkali-neutralization-induced glucan reassembly from differences in polymer composition, native β-1,3-1,6-glucan (t-glucan), the direct precursor of r-glucan NPs, was included as a composition-matched control. The encapsulation state of quercetin was characterized by UV–visible absorption spectroscopy, circular dichroism spectroscopy, and dynamic light scattering. We further compared the apparent aqueous dispersibility, ORAC-based antioxidant capacity, photostability, pH-dependent stability, cytocompatibility, and cellular antioxidant activity of free quercetin, the quercetin/β-CD complex, and quercetin-loaded r-glucan NPs. Accordingly, this study aimed to determine whether r-glucan NPs provide functional advantages over β-CD as a structurally simple and food-compatible carrier for quercetin in aqueous nutraceutical formulations.

2. Materials and Methods

2.1. Materials

Quercetin, acetone, methanol, 99.5% ethanol, ethyl acetate, dipotassium hydrogen phosphate, potassium dihydrogen phosphate, acetic acid, hydrochloric acid, fluorescein, Trolox, 2,2′-azobis(2-amidinopropane) dihydrochloride (AAPH), sodium hydroxide, phenol, sulfuric acid, 3-(4,5-Dimethyl-2-thiazolyl)-2,5-diphenyl-2H-tetrazolium bromide (MTT), Hank's balanced salt solution (HBSS) (−) without phenol red, Dulbecco's modified Eagle's medium (DMEM), fetal bovine serum (FBS), penicillin–streptomycin, phosphate-buffered saline (PBS), and trypsin–EDTA were purchased from Fujifilm Wako Chemicals Co., Ltd. (Osaka, Japan). β-Cyclodextrin (β-CD) was purchased from Tokyo Chemical Industry Co., Ltd. (Tokyo, Japan). 2′,7′-Dichlorodihydrofluorescein diacetate (DCFH-DA) was pur-

chased from Sigma-Aldrich (St. Louis, MO, USA). All reagents were used without further purification unless otherwise stated.

2.2. β-1,3-1,6-Glucan

β-1,3-1,6-Glucan was obtained by fermentation of the K-1 strain of *Aureobasidium pullulans* according to a previously reported method [19]. The *A. pullulans* K-1 strain was kindly provided by Prof. T. Suzuki. The molecular-weight parameters of the obtained β-1,3-1,6-glucan were estimated to be M_w = 1,880,000, M_n = 35,600, and M_w/M_n = 52.7, as determined by gel permeation chromatography (GPC) [19]. Previous GPC analyses showed that native β-1,3-1,6-glucan and the resulting r-glucan retained broadly comparable high-molecular-weight characteristics after alkali-neutralization [19]. Consistent with this observation, the starting t-glucan and the water-dispersible r-glucan NP fraction used in the present study remained within the same high-molecular-weight range, although the r-glucan NP fraction showed a moderately lower M_w and lower dispersity than the starting t-glucan, as described below.

2.3. Preparation of Alkali-Neutralization-Induced β-1,3-1,6-Glucan Nanoparticles (r-Glucan NPs)

Alkali-neutralization-induced β-1,3-1,6-glucan nanoparticles, hereafter referred to as r-glucan NPs, were prepared according to a previously reported method [19]. β-1,3-1,6-Glucan was dissolved in 1.0 M aqueous NaOH at a glucan mass concentration of 6 wt% to dissociate its native triple-helical structure into single chains. The insoluble fraction was removed by centrifugation at 16,000× *g* for 20 min at 25 °C. The resulting alkaline solution was neutralized by adding an equivalent volume of 1.0 M aqueous HCl, and the mixture was stirred at room temperature for 1 day to allow renaturation and nanoparticle formation. The obtained suspension was dialyzed against distilled water for 1 day using a dialysis membrane with a molecular weight cut-off of 14,000 Da (ASONE, Osaka, Japan). Gel-like glucan aggregates formed during neutralization and dialysis were then removed by centrifugation at 16,000× *g* for 20 min at 25 °C, yielding a stock dispersion of r-glucan NPs. The concentration of r-glucan NPs in the stock dispersion was determined as the glucose unit concentration using the phenol–sulfuric acid method [26]. The molecular-weight parameters of the glucan chains constituting the obtained r-glucan NPs were estimated to be M_w = 1,250,000, M_n = 58,800, and M_w/M_n = 21.2, as determined by GPC.

2.4. Preparation of Quercetin-Loaded r-Glucan NPs

An aqueous dispersion of r-glucan NPs was prepared at a glucose unit concentration of 1.0 mM in a volume of 900 μL. To this dispersion, 100 μL of a 50 mM quercetin solution in acetone was added, giving a final acetone content of 10 vol%. The mixture was vortexed and then incubated at room temperature for 3 h under light-protected conditions, with vortex mixing every 60 min. After incubation, the dispersion was centrifuged at 11,000× *g* for 10 min at 25 °C to remove precipitated unencapsulated quercetin. The supernatant was collected, and an 800 μL aliquot was freeze-dried under reduced pressure (FDU-1200, EYELA, Tokyo, Japan) to remove both water and acetone. The freeze-dried sample was then redispersed in 800 μL of distilled water and centrifuged again at 11,000× *g* for 10 min at 25 °C to remove quercetin that had been solubilized in the initial acetone-containing medium but was not stably retained in the r-glucan NP system after solvent removal. The resulting supernatant was used as the quercetin-loaded r-glucan NP sample.

2.5. Preparation of the Quercetin-Treated Native β-1,3-1,6-Glucan Control

Native β-1,3-1,6-glucan (t-glucan), the precursor of r-glucan NPs, was examined as a control. An aqueous dispersion of t-glucan was prepared at a glucose-unit concentration of 1.0 mM in a volume of 900 μL. Quercetin was added and processed under the same

conditions used for r-glucan NPs, including the addition of 100 μL of 50 mM quercetin in acetone, incubation for 3 h, centrifugation, freeze-drying, redispersion in distilled water, and a second centrifugation. The resulting supernatant was used as the quercetin-treated native β-1,3-1,6-glucan control.

2.6. Quantification of Quercetin Retained in Glucan Samples

The amount of quercetin encapsulated in r-glucan NPs and the apparent amount of quercetin retained by t-glucan were quantified by alkaline dissociation of the glucan assemblies followed by UV–visible absorption spectroscopy, based on a guest-quantification method previously established for r-glucan NPs [22]. An aliquot of the final aqueous supernatant obtained as described in Section 2.4 or Section 2.5 was mixed with an equal volume of 2.0 M aqueous NaOH and allowed to stand for 3 h at room temperature under light-protected conditions. This treatment dissociated the r-glucan NP structure and released carrier-associated quercetin into solution. For the t-glucan control, the same alkaline treatment was applied to solubilize the glucan and release the retained quercetin. The UV–visible absorption spectrum was recorded using a UV-1800 spectrophotometer (Shimadzu, Kyoto, Japan). The quercetin concentration was calculated from a calibration curve prepared using quercetin in 1.0 M aqueous NaOH. Quercetin loading was expressed as the mole fraction of quercetin relative to the total molar amounts of quercetin and carrier glucose units. Three independently prepared samples were analyzed, and the results are presented as mean ± standard deviation (SD).

2.7. Preparation of the Quercetin/β-CD Complex

The quercetin/β-CD complex was prepared by ultrasound-assisted solid–liquid equilibration, with modifications from previously reported phase-solubility procedures using excess solid guest compounds and aqueous β-CD solutions [27]. β-CD was dissolved in distilled water, and the total glucose unit concentration of the β-CD solution was determined using the phenol–sulfuric acid method. The solution was then diluted with distilled water to a glucose unit concentration of 1.0 mM. An excess amount of quercetin (200 mg) was added to the β-CD solution (50 mL). The mixture was vortexed for 10 s and sonicated for 1 h under ice-cooling using an ultrasonic homogenizer (UH-50, SMT Co., Ltd., Tokyo, Japan). After sonication, the suspension was centrifuged at 11,000× *g* for 10 min at 25 °C to remove uncomplexed quercetin. The resulting supernatant was collected and freeze-dried using a freeze dryer (FDU-1200, EYELA, Tokyo, Japan). The obtained freeze-dried powder was used as the quercetin/β-CD complex in subsequent experiments.

2.8. Quantification of Quercetin Incorporated into β-CD

The amount of quercetin incorporated into β-CD was quantified by UV–visible absorption spectroscopy using an ethanol-based calibration curve. The analytical procedure was adapted, with modifications, from previous studies of cyclodextrin inclusion complexes [28,29]. To determine the total amount of quercetin present in the freeze-dried quercetin/β-CD sample, the powder prepared at a total glucose unit concentration of 1.0 mM was dissolved in ethanol. The UV–visible absorption spectrum was measured using a 1.0 cm quartz cell, and the total amount of quercetin was calculated from the calibration curve. Separately, the amount of water-insoluble, uncomplexed quercetin was determined. The freeze-dried quercetin/β-CD sample was redissolved in distilled water and centrifuged at 11,000× *g* for 10 min at 25 °C. After removal of the supernatant, the remaining precipitate was dissolved in ethanol. The UV–visible absorption spectrum was measured, and the amount of uncomplexed quercetin was calculated from the ethanol calibration curve. The amount of quercetin incorporated into β-CD was calculated by subtracting the amount of water-insoluble quercetin from the total amount of quercetin present

in the freeze-dried sample. For the β-CD formulation, quercetin loading was expressed as its mole fraction relative to the total molar amounts of quercetin and β-CD glucose-unit equivalents, using the same equation described in Section 2.6.

2.9. UV–Visible Absorption and Circular Dichroism Spectroscopy

UV–visible absorption and circular dichroism (CD) spectra of free quercetin, the quercetin-treated t-glucan control, the quercetin/β-CD complex, and quercetin-loaded r-glucan NPs were measured to evaluate the initial encapsulation or association state of quercetin in each system. Free quercetin was dissolved directly in distilled water at a concentration of 3.47 μM. The quercetin-treated t-glucan control, the quercetin/β-CD complex, and quercetin-loaded r-glucan NPs were prepared in distilled water and adjusted to a quercetin concentration of 150 μM on a quercetin basis. The quercetin-treated t-glucan sample was measured immediately after the final centrifugation to characterize its initial association state under distilled-water conditions. UV–visible absorption spectra were recorded over the wavelength range of 230–500 nm using a UV-1800 spectrophotometer (Shimadzu, Kyoto, Japan) with a quartz cell of 1.0 mm path length. CD spectra were recorded over the same wavelength range using a JASCO J-820 spectropolarimeter (JASCO, Tokyo, Japan) equipped with a temperature controller and a quartz cell of 1.0 cm path length. All measurements were performed at 25 °C. Each CD spectrum was obtained by averaging three scans. Distilled water was used as the blank for baseline correction.

2.10. Dynamic Light Scattering Measurements

Dynamic light scattering (DLS) measurements were performed to evaluate the hydrodynamic size distributions of blank r-glucan NPs, blank native β-1,3-1,6-glucan (t-glucan), the quercetin-treated t-glucan control, the quercetin/β-CD complex, and quercetin-loaded r-glucan NPs. Measurements were carried out using a Zetasizer Nano ZS instrument (Malvern Panalytical Ltd., Worcestershire, UK) equipped with a temperature controller. Samples were dispersed in distilled water and measured at 25 °C using disposable polystyrene cuvettes with a 1 cm path length. Before measurement, the samples were equilibrated at 25 °C for 2 min. The supernatants obtained after centrifugation at 11,000× *g* for 10 min at 25 °C were used for DLS measurements without further filtration. The concentrations of blank r-glucan NPs and quercetin-loaded r-glucan NPs were adjusted to 4.0% (*w*/*v*) on a glucan basis. The quercetin/β-CD complex was measured as a saturated aqueous solution prepared at a β-CD concentration of 1.0% (*w*/*v*). Blank t-glucan and the quercetin-treated t-glucan control were measured at a glucose-unit concentration of 2.2 mM (0.036%). Because 1 vol% ethanol was included in the subsequent release/retention, photostability, and pH-dependent stability assays as a minimal cosolvent to facilitate sample preparation at the measurement concentration and reduce rapid precipitation of quercetin, the dispersion behavior of the quercetin-treated t-glucan control was also examined under the same solvent condition. DLS measurements were performed in distilled water and immediately after the addition of ethanol to a final concentration of 1 vol%. The polydispersity index (PDI) was obtained by cumulants analysis using the instrument software, whereas size distributions and mean hydrodynamic diameters are presented on a number-weighted basis. For blank r-glucan NPs, the quercetin/β-CD complex, and quercetin-loaded r-glucan NPs, three independently prepared samples were analyzed. Each preparation was measured 30 times, and the mean value obtained for each preparation was used to calculate the overall mean ± SD ($n = 3$). For blank t-glucan, the values represent the mean ± SD of 10 consecutive technical measurements of one representative preparation. For the quercetin-treated t-glucan control in distilled water and after the addition of 1 vol% ethanol, the values represent the mean ± SD of 30 consecutive technical measurements of a

representative preparation under each condition. These consecutive measurements were used to characterize the dispersion states and were not treated as independent experimental replicates. After the initial DLS measurement, the ethanol-containing quercetin-treated t-glucan sample was stored at 25 °C under light-protected conditions and visually inspected periodically over 3 days for the development of turbidity and precipitation.

2.11. Apparent Aqueous Solubility/Dispersibility Test

The apparent aqueous solubility or dispersibility of free quercetin, the quercetin/β-CD complex, and quercetin-loaded r-glucan NPs was evaluated by a stepwise addition method. For the quercetin-treated t-glucan control, only the apparent saturation-point value was determined. A complete concentration–addition profile was not generated because repeated cycles of powder addition, mixing, centrifugation, and measurement using the same sample produced unstable and poorly reproducible aqueous quercetin concentrations. Instead, the formulation was added to water until visible undispersed material remained, after which the supernatant was collected by centrifugation under the same conditions and used to determine the apparent saturated quercetin concentration. For free quercetin, the quercetin/β-CD complex, and quercetin-loaded r-glucan NPs, distilled water (1.0 mL) was added to a 1.5 mL plastic tube, followed by the addition of 10 mg of the corresponding sample. The mixture was vortexed to dissolve or disperse the sample. When the sample was completely dissolved or dispersed, an additional 10 mg portion was added, and the same procedure was repeated until undissolved material remained. The resulting mixture was centrifuged at 11,000× *g* for 10 min at 25 °C, and the supernatant was collected. The collected supernatant was centrifuged again under the same conditions to remove any remaining insoluble material. For free quercetin and the quercetin/β-CD complex, a 100 μL aliquot of the final supernatant was mixed with 900 μL of ethanol, and the mixture was vortexed. The UV–visible absorption spectrum was recorded, and the apparent saturated quercetin concentration was determined from the absorbance at the absorption maximum of quercetin using a calibration curve prepared in ethanol. For the quercetin-treated t-glucan control and quercetin-loaded r-glucan NPs, a 100 μL aliquot of the final supernatant was mixed with 100 μL of 2.0 M aqueous NaOH. The mixture was allowed to stand for 3 h at room temperature under light-protected conditions to solubilize or dissociate the glucan assemblies and release the associated quercetin. The apparent saturated quercetin concentration was then determined using a calibration curve prepared in 1.0 M aqueous NaOH.

2.12. ORAC Assay

The oxygen radical absorbance capacity (ORAC) assay was selected because it evaluates the ability of antioxidants to suppress AAPH-generated peroxyl radicals under aqueous, near-physiological pH conditions and incorporates both the magnitude and duration of radical-scavenging activity. It was therefore considered suitable for comparing free and carrier-associated quercetin in aqueous formulations. The ORAC assay was conducted according to the hydrophilic ORAC method reported by Watanabe et al. with minor modifications [30]. ORAC values were determined using Trolox as the standard antioxidant.

Two complementary comparisons were performed. First, free quercetin, the quercetin/β-CD complex, and quercetin-loaded r-glucan NPs were compared at a fixed quercetin concentration of 5.0 μM to evaluate antioxidant activity on an equal-quercetin basis. Second, concentration-dependent ORAC values were determined within the experimentally accessible aqueous concentration range of each formulation. The highest experimentally obtained ORAC value within this range was defined as the maximum experimentally observed ORAC value under the present aqueous assay conditions.

Samples were diluted with assay buffer consisting of 75 mM phosphate buffer (pH 7.4). Trolox standard solutions were prepared at concentrations of 6.25, 12.5, 25, and 50 μM in the same assay buffer. A 35 μL aliquot of the diluted sample solution or Trolox standard solution was added to each well of a 96-well plate. Subsequently, 115 μL of fluorescein solution (110.7 nM) and 50 μL of AAPH solution (31.7 mM) were added to each well. The plate was covered with a plate seal to prevent evaporation and incubated at 37 °C. Fluorescence intensity was monitored every 2 min for 90 min using a microplate reader (Thermo Fisher Scientific Inc., Waltham, MA, USA) at an excitation wavelength of 485 nm and an emission wavelength of 528 nm. The area under the curve (AUC) of the fluorescence decay curve from 8 to 90 min after addition of AAPH was calculated for each well. The net AUC was calculated by subtracting the AUC of the blank from that of the sample or Trolox standard. A calibration curve was prepared from the net AUC values of the Trolox standard solutions, and the antioxidant capacity of each sample was expressed as Trolox equivalents. Carrier-only controls consisting of blank r-glucan NPs and β-CD were measured at the same carrier concentrations as those present in the corresponding quercetin formulations. Their ORAC values were evaluated separately and were not subtracted from those of the corresponding quercetin formulations because such subtraction would assume that the effects of the carrier and quercetin on the fluorescence decay kinetics were independent and additive.

2.13. Apparent Release/Retention Assay of Quercetin from Carrier Systems

The apparent release or retention behavior of quercetin from the quercetin/β-CD complex and quercetin-loaded r-glucan NPs was evaluated in aqueous solution containing 1 vol% ethanol. The quercetin concentration of each sample was adjusted to 25 μM on a quercetin basis. Each sample solution was added to a 96-well glass plate at 250 μL per well and incubated at 37 °C under light-protected conditions. UV–visible absorption spectra were recorded at 1 h intervals using a Varioskan LUX microplate reader (Thermo Fisher Scientific Inc., Waltham, MA, USA). The residual fraction of carrier-associated quercetin was calculated from the absorbance at the absorption maximum of each sample at each time point relative to the initial absorbance at 0 h. The apparent release/retention behavior was analyzed by plotting the residual fraction of carrier-associated quercetin as a function of incubation time. When appropriate, the apparent rate constant for the decrease in carrier-associated quercetin was determined from the slope of the linear plot of $\ln(A_t/A_0)$ versus incubation time, where A_t and A_0 represent the absorbance values of quercetin at time t and 0 h, respectively. All measurements were performed in triplicate, and the data are presented as mean ± SD.

2.14. Photodegradation Assay of Free and Encapsulated Quercetin

The photostability of free quercetin, the quercetin/β-CD complex, and quercetin-loaded r-glucan NPs was evaluated under fluorescent light irradiation. The quercetin concentration of each sample was adjusted to 25 μM on a quercetin basis in aqueous solution containing 1 vol% ethanol. Each sample solution was added to a 96-well plate at 300 μL per well. The plate was placed 10 cm below a fluorescent lamp (Panasonic SQ655, Panasonic Corporation, Osaka, Japan, equipped with a 26 W fluorescent lamp) and irradiated at room temperature (25 °C). UV–visible absorption spectra were recorded at 1 h intervals over 12 h using a Varioskan LUX microplate reader (Thermo Fisher Scientific Inc., Waltham, MA, USA). The residual fraction of quercetin was calculated from the absorbance at the absorption maximum of each sample at each time point relative to the initial absorbance at 0 h. The apparent photodegradation rate constant was determined from the slope of the linear plot of $\ln(A_t/A_0)$ versus irradiation time, where A_t and A_0 represent the absorbance

values of quercetin at time t and 0 h, respectively. All measurements were performed in triplicate, and the data are presented as mean ± SD.

2.15. pH-Dependent Stability Assay of Free and Encapsulated Quercetin

The pH-dependent stability of free quercetin, the quercetin/β-CD complex, and quercetin-loaded r-glucan NPs was evaluated under acidic and intestinal pH conditions. Solutions at pH 1.2 and 6.8 were prepared to represent gastric and intestinal pH conditions, respectively. The pH 1.2 solution was prepared by dissolving NaCl (1.0 g) in approximately 400 mL of distilled water, adjusting the pH with HCl, and then diluting the solution to 500 mL. The pH 6.8 solution was prepared by dissolving KH_2PO_4 (3.40 g) in approximately 400 mL of distilled water, adjusting the pH with NaOH, and then diluting the solution to 500 mL. The pH values of the samples were measured using a LAQUA twin compact pH meter (HORIBA, Kyoto, Japan), calibrated with standard buffer solutions before use. Each sample was diluted to a final quercetin concentration of 25 μM on a quercetin basis. The final solvent composition was pH solution/water/ethanol = 89/10/1 ($v/v/v$). Each sample solution was added to a 96-well glass plate at 250 μL per well. To minimize evaporation during incubation at 37 °C, each well was overlaid with liquid paraffin. UV–visible absorption spectra were recorded at 1 h intervals over 12 h using a Varioskan LUX microplate reader (Thermo Fisher Scientific Inc., Waltham, MA, USA). The residual fraction of quercetin was calculated from the absorbance at the absorption maximum of each sample at each time point relative to the initial absorbance at 0 h. The apparent degradation rate constant was determined from the slope of the linear plot of $\ln(A_t/A_0)$ versus incubation time, where A_t and A_0 represent the absorbance values of quercetin at time t and 0 h, respectively. All measurements were performed in triplicate, and the data are presented as mean ± SD.

2.16. Evaluation of AAPH-Induced Degradation of Glucan Chains Analyzed by GPC

To evaluate whether peroxyl radicals cleave the glucan chains constituting r-glucan NPs, AAPH-induced degradation of r-glucan was analyzed by GPC. An r-glucan NP stock dispersion was prepared in distilled water, and its concentration was determined as the glucose unit concentration using the phenol–sulfuric acid method. The obtained stock dispersion had a glucose unit concentration of 95 mM and was diluted with distilled water to 40 mM. The r-glucan dispersion (40 mM on a glucose-unit basis, 25 mL) was transferred to a 50 mL plastic tube. Separately, a 40 mM AAPH solution was freshly prepared using distilled water prewarmed to 37 °C. The AAPH solution (25 mL) was added to the r-glucan dispersion and mixed, giving final concentrations of 20 mM r-glucan, on a glucose unit basis, and 20 mM AAPH. The mixture was incubated at 37 °C to generate peroxyl radicals from AAPH. An aliquot was collected immediately after mixing as the 0 h sample, and additional aliquots were collected after 3, 5.5, 23, and 48 h of incubation. Each aliquot was immediately frozen to stop further reaction. After all samples had been collected, the frozen aliquots were lyophilized. Each freeze-dried sample was redissolved in 5 mL of 0.7 M aqueous NaOH, and the molecular-weight distribution and weight-average molecular weight (M_w) of the glucan chains were analyzed by GPC as reported previously [19].

2.17. Cell Culture

Caco-2 cells were obtained from ATCC (HTB-37, Manassas, VA, USA) and cultured in DMEM supplemented with 10% FBS and 1% penicillin–streptomycin, based on established Caco-2 cell culture procedures [31]. Cells were maintained at 37 °C in a humidified atmosphere containing 5% CO_2. The culture medium was replaced every 2–3 days, and the cells were subcultured before reaching full confluence using trypsin–EDTA.

2.18. Cytotoxicity Assay in Caco-2 Cells

The cytotoxicity of free quercetin, the quercetin/β-CD complex, and quercetin-loaded r-glucan NPs toward Caco-2 cells was evaluated using an MTT assay with modifications to a previously reported method [32]. Caco-2 cells were seeded in 96-well plates at a density of 5.0×10^3 cells per well in 100 μL of complete culture medium and incubated for 24 h at 37 °C in a humidified atmosphere containing 5% CO_2. After preculture, the medium was replaced with 100 μL of fresh culture medium containing free quercetin, quercetin/β-CD complex, or quercetin-loaded r-glucan NPs at final quercetin concentrations of 0, 7.5, 15, 30, 45, 60, 75, and 100 μM. Free quercetin was added from a stock solution prepared in DMSO, whereas the quercetin/β-CD complex and quercetin-loaded r-glucan NPs were added as aqueous solutions. The final DMSO concentration was kept constant at 0.1% in the free-quercetin-treated wells and the corresponding vehicle-control wells. After exposure to the samples for 24 h, 10 μL of MTT solution (5.0 mg mL^{-1} in PBS) was added to each well, and the cells were incubated for an additional 4 h at 37 °C. The culture medium was then removed, and the wells were washed once with 200 μL of PBS. The resulting formazan crystals were dissolved in 200 μL of DMSO. After shaking the plate for 1 min, absorbance was measured at 535 nm using a Varioskan LUX microplate reader (Thermo Fisher Scientific Inc., Waltham, MA, USA). Cell viability was calculated relative to untreated control cells using the following Equation (1):

$$\text{Cell viability (\%)} = [(A_{\text{sample}} - A_{\text{blank}})/(A_{\text{control}} - A_{\text{blank}})] \times 100 \quad (1)$$

where A_{sample}, A_{control}, and A_{blank} represent the absorbance values of sample-treated wells, untreated control wells, and blank wells without cells, respectively. Measurements were performed in triplicate, and the data are presented as mean ± SD.

2.19. Cellular Antioxidant Activity (CAA) Assay

Cellular antioxidant activity (CAA) was evaluated in Caco-2 cells using an AAPH-induced oxidative stress model according to a previously reported method [33,34]. Caco-2 cells were seeded in black 96-well plates at a density of 5.0×10^4 cells per well in 100 μL of culture medium and precultured for 24 h at 37 °C under a humidified atmosphere containing 5% CO_2. After preculture, the medium was removed, and the cells were washed once with PBS. Then, 100 μL of serum-free DMEM containing 60 μM DCFH-DA and each sample, namely free quercetin, the quercetin/β-CD complex, or quercetin-loaded r-glucan NPs, was added to each well at final quercetin concentrations of 0, 10, 20, 30, 40, and 50 μM. The cells were incubated for 20 min at 37 °C. After incubation, the reaction solution was removed, and the cells were washed again with PBS. Oxidative stress was induced by adding 100 μL of HBSS containing 500 μM AAPH to each well. For blank wells, HBSS without AAPH was added instead. Fluorescence intensity was immediately monitored using a Varioskan LUX microplate reader (Thermo Fisher Scientific Inc., Waltham, MA, USA) at an excitation wavelength of 485 nm and an emission wavelength of 535 nm every 5 min for 90 min at 37 °C. The area under the fluorescence intensity–time curve (AUC) was calculated, and cellular antioxidant activity was evaluated using the following Equation (2):

$$\text{CAA (\%)} = [1 - (\text{AUC}_{\text{sample}} - \text{AUC}_{\text{blank}})/(\text{AUC}_{\text{AAPH control}} - \text{AUC}_{\text{blank}})] \times 100 \quad (2)$$

where $\text{AUC}_{\text{sample}}$ is the area under the fluorescence curve of cells treated with each quercetin formulation in the presence of AAPH, $\text{AUC}_{\text{AAPH control}}$ is that of cells treated with AAPH in the absence of quercetin, and $\text{AUC}_{\text{blank}}$ is that of cells treated with HBSS without AAPH. Measurements were performed in triplicate, and the data are presented as mean ± SD.

2.20. Statistical Analysis

Unless otherwise stated, data are presented as mean ± SD from three independent experiments. The apparent rate constants for the loss of carrier-associated quercetin from the r-glucan NP and β-CD formulations were compared using Welch's two-tailed *t*-test. For the apparent photodegradation and pH-dependent degradation rate constants, differences among the three formulations were analyzed by one-way analysis of variance (ANOVA) followed by Tukey's honestly significant difference (HSD) multiple-comparison test. For the pH-dependent stability assay, the comparisons were performed separately at pH 1.2 and 6.8. For the fixed-concentration ORAC assay and the MTT and CAA assays, differences among free quercetin, quercetin-loaded r-glucan NPs, and the quercetin/β-CD complex at each quercetin concentration were analyzed by one-way ANOVA, followed by Tukey's HSD multiple-comparison test. A value of $p < 0.05$ was considered statistically significant. Statistical analyses were performed using Microsoft Excel for Mac (version 16.111.1) with the Real Statistics Resource Pack (version 9.8).

3. Results and Discussion

3.1. Preparation and Characterization of Quercetin-Loaded r-Glucan NPs

Quercetin-loaded r-glucan NPs were prepared by adding an acetone stock solution of quercetin to an aqueous dispersion of r-glucan NPs at a final acetone content of 10 vol%. Under these conditions, poorly water-soluble quercetin was expected to partition into hydrophobic cavity-like microenvironments formed within the r-glucan NPs. After incubation, precipitated unencapsulated quercetin was removed by centrifugation, and the supernatant was freeze-dried to remove water and acetone. The dried material was subsequently redispersed in distilled water and centrifuged again to remove quercetin that had been solubilized only in the initial acetone-containing medium but was not retained after solvent removal and redispersion. Therefore, the quercetin detected in the final aqueous dispersion was regarded as the fraction retained by r-glucan NPs after completion of the preparation process.

The amount of quercetin incorporated into r-glucan NPs was quantified using the same method previously employed for curcumin quantification [22]. Briefly, the glucan nanoparticle structure was dissociated under alkaline conditions to release the encapsulated quercetin into solution, after which the quercetin concentration was determined. The mole fraction of quercetin in quercetin-loaded r-glucan NPs was 2.42 ± 0.41 mol%. To determine whether the retention of quercetin was attributable to alkali-neutralization-induced reassembly of β-1,3-1,6-glucan rather than to the native glucan itself, native β-1,3-1,6-glucan (t-glucan) was examined under the same quercetin-loading conditions. Because t-glucan and r-glucan have the same polysaccharide composition and both consist of high-molecular-weight glucan chains, t-glucan served as a composition-matched precursor control for evaluating the effect of glucan-chain reassembly. The apparent mole fraction of quercetin retained in the freshly prepared aqueous t-glucan fraction was 2.16 ± 0.03 mol%, compared with 2.42 ± 0.41 mol% for quercetin-loaded r-glucan NPs. Thus, native t-glucan initially retained an appreciable amount of quercetin under the present preparation conditions. The freshly prepared quercetin-treated t-glucan sample appeared macroscopically dispersed in distilled water and could therefore be analyzed immediately by UV–visible absorption and CD spectroscopy.

DLS measurements were performed to characterize blank and quercetin-treated t-glucan. The number-weighted mean hydrodynamic diameters were 15.8 ± 6.1 nm for blank t-glucan and 28.2 ± 19.4 nm after quercetin treatment, although considerable variation was observed among consecutive measurements. This variability suggested that the dispersed t-glucan fraction was heterogeneous. In the sample containing 1 vol% ethanol, the mean

diameter was 17.8 ± 11.7 nm immediately after ethanol addition (Figure S1a), and the sample appeared relatively homogeneous (Figure S1b). However, it gradually became turbid and formed a visible precipitate after 3 days (Figure S1c), indicating insufficient dispersion stability under the conditions used in the subsequent assays. Therefore, t-glucan was used as a control for initial quercetin retention, spectroscopic characterization, and dispersion-state analysis, but not for longer-term release/retention, photostability, or pH-dependent stability assays.

For comparison with a representative low-molecular-weight host system, the quercetin/β-CD complex was prepared, and its quercetin loading was determined to be 0.77 ± 0.03 mol% on a glucose-unit-equivalent basis. The quercetin loading of r-glucan NPs was therefore approximately 3.1-fold higher than that of the quercetin/β-CD complex. This result indicates that r-glucan NPs provided a higher effective incorporation capacity for quercetin than β-CD under the present preparation conditions. The difference between r-glucan NPs and β-CD may be related to their distinct host architectures. β-CD provides a single, relatively rigid molecular cavity, whereas r-glucan NPs possess a polymeric and supramolecular structure containing multiple hydrophobic cavity-like regions generated during glucan-chain reassembly. These broader and more flexible microenvironments may accommodate and retain a larger amount of quercetin than the discrete cavity of β-CD.

The encapsulation or association state of quercetin was first examined by UV–visible absorption spectroscopy (Figure 1a). Quercetin exhibits two characteristic absorption regions, designated as Band II in the short-wavelength region and Band I in the long-wavelength region. Free quercetin showed a Band I absorption maximum at 368 nm, whereas the quercetin/β-CD complex showed a similar maximum at 367 nm. The quercetin fraction retained by native t-glucan also exhibited a Band I maximum at 366 nm. Thus, neither β-CD complexation nor association with native t-glucan substantially affected Band I of quercetin. In contrast, quercetin-loaded r-glucan NPs exhibited a bathochromic shift in the Band I maximum to 372 nm. This shift indicates that the electronic environment responsible for Band I was altered within the r-glucan NP assemblies. The difference between t-glucan and r-glucan NPs suggests that alkali-neutralization-induced reassembly generated microenvironments that were not present in the native glucan structure.

Further information on the encapsulation or association state of quercetin was obtained from CD spectroscopy (Figure 1b). Free quercetin showed no appreciable CD signal, as expected for an achiral chromophore in solution. The quercetin/β-CD complex exhibited an induced CD (ICD) signal mainly in the Band II region around 270 nm, whereas no clear ICD signal was observed in the Band I region around 370 nm. This spectral feature suggests that the chromophoric region contributing predominantly to Band II was affected by the chiral environment of β-CD, whereas the chromophore contributing to Band I was not strongly influenced by the β-CD cavity. The absence of a clear ICD signal in the Band I region is therefore consistent with a partial inclusion mode rather than complete accommodation of the quercetin aromatic framework within the β-CD cavity.

The quercetin fraction retained by native t-glucan showed only a weak and poorly defined CD response, with no well-resolved ICD signal in the Band I region. Together with its Band I maximum at 366 nm, this result provides little evidence that quercetin was immobilized within a well-defined chiral microenvironment. These spectra were recorded immediately after preparation in distilled water and therefore describe the initial association state of quercetin with t-glucan.

In contrast, the CD spectrum of quercetin-loaded r-glucan NPs was markedly different from those of the quercetin/β-CD complex and the quercetin-treated t-glucan control. A more pronounced CD response was observed not only in the Band II region around 270 nm but also in the Band I region around 370 nm. This indicates that a broader portion of the

quercetin chromophore was influenced by the chiral environment of the β-1,3-1,6-glucan framework. Although the exact origin of the CD response in the Band I region cannot be assigned solely from the present spectra, local interactions between quercetin and the chiral β-1,3-1,6-glucan framework are considered more plausible than intermolecular exciton coupling between quercetin molecules at the concentration used for the CD measurement (150 μM). Thus, these observations are consistent with the association of the Band I chromophore with chiral microenvironments within the cavity-rich domains of r-glucan NPs, although the exact binding geometry cannot be determined from the present CD data alone.

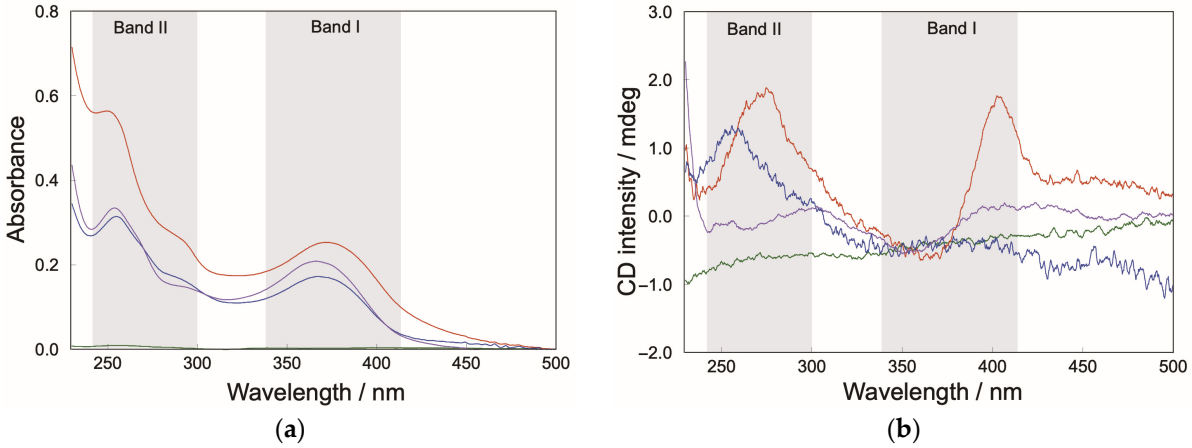

Figure 1. UV–visible absorption and circular dichroism spectra of free and carrier-associated quercetin. (**a**) UV–visible absorption spectra and (**b**) circular dichroism (CD) spectra of free quercetin, the quercetin-treated native β-1,3-1,6-glucan (t-glucan) control, quercetin-loaded renatured β-1,3-1,6-glucan nanoparticles (r-glucan NPs), and the quercetin/β-cyclodextrin (β-CD) complex. Free quercetin, the quercetin-treated t-glucan control, quercetin-loaded r-glucan NPs, and the quercetin/β-CD complex are shown in green, purple, red, and blue, respectively. The shaded regions indicate the characteristic Band II and Band I regions of quercetin. The Band I absorption maxima were 368, 366, 372, and 367 nm, and the principal Band II absorption maxima were 253, 254, 249, and 255 nm for free quercetin, the quercetin-treated t-glucan control, quercetin-loaded r-glucan NPs, and the quercetin/β-CD complex, respectively. Only the principal Band II maximum was assigned because additional shoulder features were not sufficiently resolved for reliable peak identification. The quercetin concentrations were 3.47 μM for free quercetin and 150 μM, on a quercetin basis, for each carrier-associated formulation. Because different concentrations were required owing to the limited aqueous solubility of free quercetin, comparisons involving free quercetin are intended primarily as qualitative comparisons of spectral features.

DLS measurements were then performed to evaluate how quercetin incorporation affected the dispersion states of the carrier systems (Figure S2). Blank r-glucan NPs showed a number-weighted mean hydrodynamic diameter of 11.5 ± 2.6 nm with a PDI of 0.80 ± 0.04. This result is consistent with the presence of small glucan-based nanoparticles, although the high PDI indicates that the dispersion contained a broad distribution of glucan species. After quercetin loading, the number-weighted mean hydrodynamic diameter increased to 163 ± 113 nm, with a PDI of 0.393 ± 0.036. This change suggests that quercetin incorporation substantially altered the dispersion state of r-glucan NPs.

A similar increase in particle size upon guest incorporation was observed in our previous study of curcumin-loaded r-glucan NPs, in which the number-weighted mean hydrodynamic diameter increased from 17.8 ± 5.0 to 69.6 ± 31.6 nm after curcumin incorporation [22]. This previous result suggests that r-glucan NPs can expand or swell when hydrophobic guest molecules are incorporated into their cavity-rich domains. The larger mean diameter observed for the present quercetin-loaded system, together with its

substantial variability, suggests that the dispersion may not consist solely of individually swollen nanoparticles. Quercetin incorporation may promote both expansion of the glucan nanoparticle domains and secondary association among quercetin-loaded domains.

Guest incorporation may alter the local hydration and hydrophobic interactions within and between the glucan domains, thereby contributing to secondary association of the nanoparticles. Importantly, however, the quercetin-loaded r-glucan NP sample remained dispersible in water after freeze-drying and redispersion, indicating that these larger assemblies remained macroscopically dispersed rather than forming visible precipitates.

In contrast, the quercetin/β-CD complex showed a number-weighted mean hydrodynamic diameter of 850 ± 103 nm with a PDI of 0.457 ± 0.067 (Figure S2). This result suggests that the quercetin/β-CD complex did not exist only as isolated molecular inclusion complexes in water but also formed larger secondary aggregates. This behavior may be related to the partial inclusion mode suggested by the CD spectrum. If only part of the quercetin molecule is included in the β-CD cavity, the remaining exposed aromatic region may participate in intermolecular hydrophobic or π–π interactions, thereby promoting aggregation of the quercetin/β-CD complexes.

3.2. Enhanced Apparent Aqueous Solubility/Dispersibility of Quercetin

Based on the distinct encapsulation state of quercetin in r-glucan NPs described above, we next examined whether this carrier system improved the ability of quercetin to remain in the aqueous phase. Because quercetin-loaded r-glucan NPs are dispersed as carrier-associated nanoparticle assemblies rather than dissolved as individual quercetin molecules, the obtained values are described here as apparent aqueous solubility/dispersibility. The apparent aqueous solubility/dispersibility of quercetin was evaluated by measuring the quercetin concentration in the supernatant after centrifugation following stepwise addition of each formulation to water (Figure 2). Free quercetin was also examined as a reference because of its intrinsically poor water solubility.

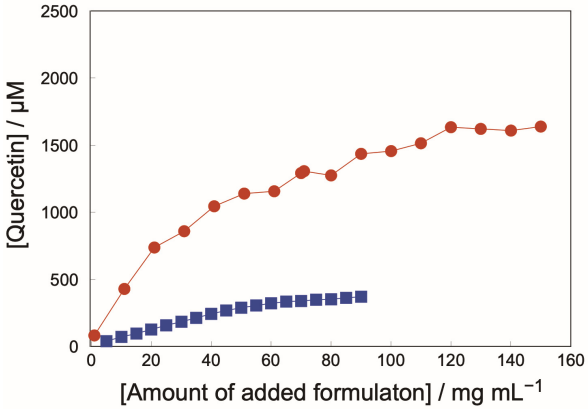

Figure 2. Apparent aqueous solubility/dispersibility of quercetin in the r-glucan NP and β-CD formulations. The quercetin concentration in the aqueous supernatant after centrifugation was plotted as a function of the amount of added formulation. Quercetin-loaded r-glucan NPs and the quercetin/β-CD complex are shown as red circles and blue squares, respectively. Data are presented as mean ± standard deviation (SD) from three independently prepared samples. For the quercetin-treated t-glucan control, only the apparent saturation-point value was determined because a reproducible concentration–addition profile could not be obtained; therefore, the t-glucan control was not included in this plot.

As shown in Figure 2, the quercetin concentration in the aqueous supernatant increased with increasing amounts of the quercetin-loaded r-glucan NP and quercetin/β-CD formulations. The apparent saturated quercetin concentration reached 1620 ± 15.3 μM

for quercetin-loaded r-glucan NPs and 347 ± 16.4 μM for the quercetin/β-CD complex. For the quercetin-treated t-glucan control, only the apparent saturation-point value was determined because repeated cycles of powder addition, mixing, centrifugation, and measurement produced unstable and poorly reproducible aqueous quercetin concentrations. Therefore, a complete concentration–addition profile was not included in Figure 2. The apparent saturated quercetin concentration of the t-glucan formulation was 256 ± 0.52 μM. In contrast, free quercetin showed an apparent aqueous solubility of only 7.11 ± 3.97 μM under the same conditions. Thus, r-glucan NPs increased the apparent aqueous solubility/dispersibility of quercetin by approximately 228-fold relative to free quercetin, 6.3-fold relative to the t-glucan control, and 4.7-fold relative to the quercetin/β-CD complex. Although t-glucan initially retained quercetin at a mole fraction comparable to that of r-glucan NPs, its lower apparent saturated quercetin concentration indicates that quercetin retention per glucose unit did not directly translate into comparable formulation-level aqueous dispersibility. These results suggest that the water-dispersible nanoparticle architecture generated by glucan-chain reassembly, rather than the polysaccharide composition alone, contributed to the improved aqueous performance of the r-glucan NP formulation.

The superior performance of r-glucan NPs is consistent with the encapsulation model proposed above. The cavity-rich domains generated during glucan reassembly may provide broader and more flexible microenvironments than the discrete cavity of β-CD, allowing a larger amount of quercetin to be retained in a water-dispersible state. In addition, the interaction of the quercetin chromophore with the chiral glucan microenvironment, as suggested by the CD spectra, may contribute to quercetin retention within the r-glucan NP assemblies. By contrast, the lower aqueous quercetin concentration in the β-CD system may be associated with partial inclusion and secondary aggregation, as suggested by the spectroscopic and DLS analyses. Representative photographs of the saturated aqueous supernatants are shown in Figure S3. The quercetin-loaded r-glucan NP sample appeared visually homogeneous and showed a more intense yellow color than the free quercetin and quercetin/β-CD samples. These visual observations are consistent with the quantitative apparent aqueous solubility/dispersibility results shown in Figure 2.

These results demonstrate that r-glucan NPs are highly effective in improving the apparent aqueous solubility/dispersibility of quercetin. This property is particularly advantageous for the use of quercetin in aqueous food, nutraceutical, and health-related formulations, where homogeneous dispersion and high functional ingredient loading are essential.

3.3. Antioxidant Capacity of Quercetin After Inclusion

3.3.1. Antioxidant Activity at a Fixed Quercetin Concentration

The results described above demonstrated that r-glucan NPs markedly increased the amount of quercetin that could be maintained in the aqueous phase. However, increased aqueous dispersibility does not necessarily mean that the antioxidant activity of quercetin is fully preserved after encapsulation, because incorporation into carrier domains may restrict the accessibility of quercetin to radical species. Therefore, we first compared the antioxidant activity of free and encapsulated quercetin at the same quercetin concentration using the ORAC assay. This assay evaluates the ability of antioxidants to suppress fluorescence decay induced by AAPH-derived peroxyl radicals and is suitable for comparing radical-scavenging activity in aqueous systems.

Figure 3 shows the ORAC values of the three formulations at a fixed quercetin concentration of 5.0 μM. The ORAC values differed significantly among all three formulations, as determined by one-way ANOVA followed by Tukey's HSD multiple-comparison test ($p < 0.05$). Free quercetin showed the highest ORAC value, followed by quercetin-loaded

r-glucan NPs and the quercetin/β-CD complex, indicating that molecularly available quercetin can efficiently scavenge peroxyl radicals in the aqueous assay medium. In contrast, the ORAC value of quercetin-loaded r-glucan NPs decreased to 51.5% of that of free quercetin. This decrease suggests that encapsulation partially restricted the direct accessibility of quercetin to peroxyl radicals. However, the quercetin/β-CD complex showed a much lower ORAC value, corresponding to only 16.5% of that of free quercetin and approximately 32% of that of quercetin-loaded r-glucan NPs. Thus, although encapsulation reduced the apparent radical-scavenging activity of quercetin in both carrier systems, r-glucan NPs retained the antioxidant activity of quercetin much more effectively than β-CD. These ORAC values should be interpreted as the apparent antioxidant capacities of the whole carrier–quercetin systems rather than as the intrinsic activity of quercetin alone. At carrier concentrations corresponding to those in the 5.0 μM quercetin formulations, blank r-glucan NPs showed a low but detectable ORAC value of 10.9 μmol TE L^{-1}, whereas β-CD was below the detectable level. Therefore, the values shown in Figure 3 represent the apparent ORAC responses of the complete formulations and were not corrected by subtraction of the carrier-only values.

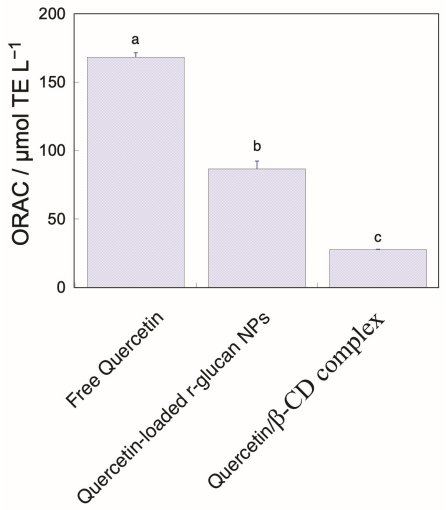

Figure 3. Oxygen radical absorbance capacity (ORAC) responses of free and carrier-associated quercetin at a fixed quercetin concentration. Free quercetin, quercetin-loaded r-glucan NPs, and the quercetin/β-CD complex were compared at a fixed quercetin concentration of 5.0 μM, on a quercetin basis. ORAC values are expressed as Trolox equivalents. The values represent the apparent ORAC responses of the complete formulations and were not corrected by subtraction of the corresponding carrier-only values. Data are presented as mean ± SD from three independent experiments. Differences among the three formulations were analyzed by one-way analysis of variance (ANOVA) followed by Tukey's honestly significant difference (HSD) multiple-comparison test. Different lowercase letters indicate significant differences among the formulations ($p < 0.05$); groups sharing at least one letter are not significantly different.

The difference between the two carrier systems is consistent with the encapsulation states discussed above. In the quercetin/β-CD complex, partial inclusion and secondary aggregation may reduce the accessibility of quercetin to AAPH-derived peroxyl radicals. By contrast, the quercetin-loaded r-glucan NP formulation retained more than half of the ORAC response of free quercetin on an equal-quercetin basis. This result suggests that quercetin remained more accessible to peroxyl radicals in the r-glucan NP formulation than in the β-CD complex. However, the present ORAC assay does not distinguish between quercetin retained within the nanoparticles and quercetin transiently released during the assay. Thus, r-glucan NPs preserved a substantially larger apparent ORAC response than β-CD complexation at the same quercetin concentration.

3.3.2. Superior Maximal Antioxidant Capacity Enabled by Enhanced Aqueous Dispersibility

The fixed-concentration ORAC assay demonstrated that the apparent radical-scavenging activity of quercetin decreased after encapsulation. However, in aqueous food and nutraceutical formulations, practical antioxidant performance is determined not only by the activity per quercetin molecule but also by the maximum amount of quercetin that can be maintained in the aqueous phase. Therefore, the concentration-dependent ORAC values of free quercetin, the quercetin/β-CD complex, and quercetin-loaded r-glucan NPs were evaluated over the concentration ranges accessible for each formulation (Figure 4). In the low-concentration region, where all three formulations could be directly compared, free quercetin showed the highest ORAC value at a given quercetin concentration. Quercetin-loaded r-glucan NPs showed a lower but still substantial ORAC response, whereas the quercetin/β-CD complex showed the lowest activity. This tendency is consistent with the fixed-concentration comparison described above, indicating that encapsulation partially reduces the accessibility of quercetin to peroxyl radicals, but that r-glucan NPs preserve the antioxidant activity of quercetin more effectively than β-CD.

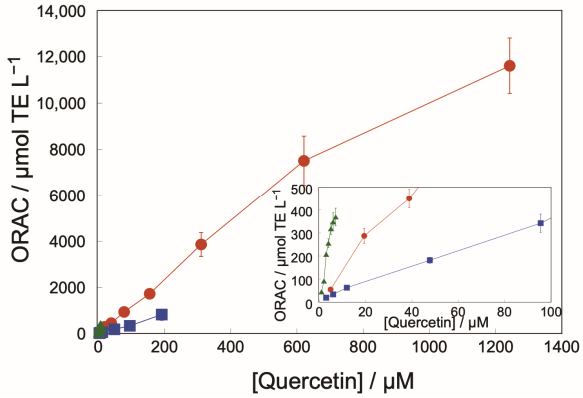

Figure 4. Concentration-dependent ORAC responses of free and carrier-associated quercetin. ORAC values of free quercetin, the quercetin/β-CD complex, and quercetin-loaded r-glucan NPs were plotted as a function of quercetin concentration, on a quercetin basis. Free quercetin, the quercetin/β-CD complex, and quercetin-loaded r-glucan NPs are shown as green triangles, blue squares, and red circles, respectively. The inset shows an expanded view of the low-concentration range in which all three formulations could be directly compared. ORAC values are expressed as Trolox equivalents. The highest value obtained within the experimentally accessible aqueous concentration range of each formulation was defined as its maximum experimentally observed ORAC value under the present assay conditions. Data are presented as mean ± SD from three independent experiments.

In contrast, comparison over the full accessible concentration range revealed a different and practically important feature. Because of its poor aqueous solubility, free quercetin could be evaluated only over a limited concentration range and reached a maximum ORAC value of 368 ± 38.2 μmol TE L^{-1} under the present aqueous conditions. The quercetin/β-CD complex increased the attainable ORAC value to 815 ± 235 μmol TE L^{-1}, corresponding to an approximately 2.2-fold improvement over free quercetin. However, this enhancement remained limited by the modest aqueous loading capacity and reduced apparent antioxidant activity of the β-CD complex. By contrast, quercetin-loaded r-glucan NPs exhibited a marked concentration-dependent increase in ORAC value over a much broader concentration range and reached a maximum ORAC value of 11,600 ± 1200 μmol TE L^{-1}. This value was approximately 32-fold higher than that of free quercetin and approximately 14-fold higher than that of the quercetin/β-CD complex. Thus, although the apparent ORAC activity of quercetin in r-glucan NPs was lower than that of free quercetin at the same quercetin concentration, the greatly enhanced aqueous dispersibility of the

r-glucan NP system more than compensated for this reduction. As a result, r-glucan NPs enabled a substantially higher total antioxidant capacity in water.

These results highlight the importance of distinguishing between molecular-level antioxidant activity and formulation-level antioxidant capacity. Free quercetin is highly active when molecularly available, but its poor aqueous solubility severely limits the maximum antioxidant capacity achievable in water. β-CD partially improves aqueous delivery, but its effect is constrained by limited incorporation capacity and reduced radical accessibility. In contrast, r-glucan NPs combine high aqueous dispersibility with retention of a substantial fraction of quercetin's radical-scavenging activity. Therefore, r-glucan NPs provide a more effective water-compatible delivery platform for maximizing the antioxidant potential of quercetin in aqueous food and nutraceutical formulations.

3.4. Sustained Retention/Release Behavior of Quercetin from r-Glucan NPs

The results described above showed that quercetin-loaded r-glucan NPs provided a much higher formulation-level antioxidant capacity in water than free quercetin and the quercetin/β-CD complex. For aqueous food and nutraceutical formulations, however, it is also important that quercetin remains in a carrier-associated and water-dispersible state over time. Therefore, we next compared the time-dependent retention of quercetin in quercetin-loaded r-glucan NPs and the quercetin/β-CD complex under aqueous conditions.

The apparent retention/release behavior was evaluated by monitoring the residual fraction of carrier-associated quercetin in aqueous solution containing 1 vol% ethanol. Because quercetin has very low aqueous solubility, quercetin lost from the carrier-associated state is expected to precipitate or form poorly dispersed aggregates in the aqueous medium. Thus, the decrease in the optically detectable quercetin signal was interpreted as the apparent loss of carrier-associated quercetin rather than as direct quercetin release. Because this absorbance-based assay cannot distinguish dissociation from precipitation, aggregation, or degradation, the results were interpreted in terms of apparent retention.

As shown in Figure 5, the residual fraction of carrier-associated quercetin gradually decreased with incubation time in both carrier systems. However, the decrease was clearly slower for quercetin-loaded r-glucan NPs than for the quercetin/β-CD complex, indicating that r-glucan NPs retained quercetin more stably under the present aqueous conditions. This result suggests that the r-glucan NP system slowed the apparent loss of quercetin from the carrier-associated state. The apparent decrease in carrier-associated quercetin was further analyzed using a pseudo-first-order kinetic model by plotting $\ln(A_t/A_0)$ against incubation time (Figure S4). The apparent rate constant for quercetin-loaded r-glucan NPs was $0.0227 \pm 0.0052\ h^{-1}$, which was significantly lower than that for the quercetin/β-CD complex ($0.0595 \pm 0.0084\ h^{-1}$; Welch's two-tailed *t*-test, $p = 0.0055$; mean ± SD, $n = 3$). Thus, the apparent loss of carrier-associated quercetin proceeded approximately 2.6 times faster in the β-CD complex than in the r-glucan NP system. This statistically significant difference quantitatively supports the greater apparent retention of quercetin of r-glucan NPs. This behavior may support sustained apparent retention in aqueous formulations.

The difference in retention behavior is likely attributable to the distinct host environments of the two carrier systems. In the β-CD complex, partial inclusion may allow relatively facile dissociation of quercetin from the β-CD cavity, and quercetin released into the aqueous phase may subsequently precipitate or form poorly dispersed aggregates because of its low water solubility. In contrast, r-glucan NPs provide hydrophobic cavity-rich microenvironments generated by the alkali-neutralization-induced reassembly of β-1,3-1,6-glucan chains. Quercetin incorporated into these domains may be stabilized through multiple interactions, including hydrophobic interactions, possible hydrogen-bonding interactions, and supramolecular organization within the glucan nanoparticle assemblies.

These features likely contribute to the slower apparent loss of carrier-associated quercetin from the r-glucan NP system.

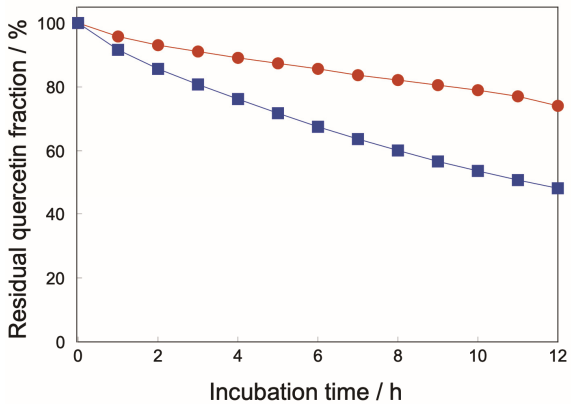

Figure 5. Apparent retention behavior of carrier-associated quercetin in aqueous media. Time-dependent changes in the residual fraction of carrier-associated quercetin in quercetin-loaded r-glucan NPs and the quercetin/β-CD complex were measured during incubation at 37 °C in aqueous solution containing 1 vol% ethanol. The initial quercetin concentration was 25 μM. Quercetin-loaded r-glucan NPs and the quercetin/β-CD complex are shown as red circles and blue squares, respectively. The residual fraction was calculated as A_t/A_0 where A_t and A_0 represent the absorbance values at time t and 0 h, respectively. A decrease in absorbance was interpreted as the apparent loss of carrier-associated quercetin and not as a direct measurement of freely dissolved or released quercetin. Data are presented as mean ± SD from three independent experiments. Statistical comparison of the apparent pseudo-first-order rate constants derived from the three independent experiments is described in the main text.

These results indicate that r-glucan NPs function not only as an aqueous dispersing carrier for quercetin but also as a retention-controlling matrix. The ability to maintain quercetin in a carrier-associated and water-dispersible state over time is expected to be advantageous for preserving quercetin functionality in aqueous food and nutraceutical formulations. However, for practical use in such formulations, it is also necessary to protect quercetin from chemical degradation during storage, processing, and exposure to gastrointestinal environments. Therefore, we next evaluated whether encapsulation in r-glucan NPs improved the stability of quercetin under light exposure and under acidic and intestinal pH conditions.

3.5. Encapsulation in r-Glucan NPs Improves the Photostability and pH-Dependent Stability of Quercetin

In addition to aqueous dispersibility and sustained retention, the chemical stability of quercetin is an important factor for its practical use in food and nutraceutical formulations. Quercetin is susceptible to degradation under light exposure and under different pH conditions [23,25]. Therefore, we evaluated the effects of encapsulation in r-glucan NPs on the photostability and pH-dependent stability of quercetin and compared the results with those of free quercetin and the quercetin/β-CD complex.

The photodegradation behavior of free and encapsulated quercetin was first examined under fluorescent light irradiation (Figure 6). In all samples, the residual quercetin fraction gradually decreased with irradiation time, indicating progressive photodegradation. However, the quercetin-loaded r-glucan NP system retained a larger fraction of quercetin than free quercetin and the quercetin/β-CD complex throughout the measurement period. In contrast, the quercetin/β-CD complex showed only limited improvement compared with free quercetin under the present conditions. These results indicate that encapsulation in r-glucan NPs effectively suppressed the photodegradation of quercetin.

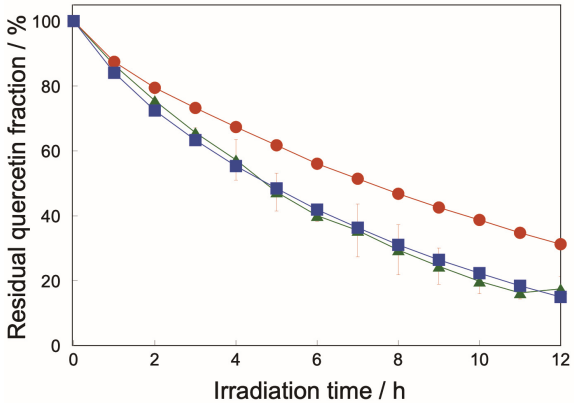

Figure 6. Photodegradation profiles of free and carrier-associated quercetin. Time-dependent changes in the residual quercetin fraction of free quercetin, quercetin-loaded r-glucan NPs, and the quercetin/β-CD complex were measured during fluorescent-light irradiation at 25 °C. The initial quercetin concentration was 25 μM in aqueous solution containing 1 vol% ethanol. Free quercetin, quercetin-loaded r-glucan NPs, and the quercetin/β-CD complex are shown as green triangles, red circles, and blue squares, respectively. The residual fraction was calculated as A_t/A_0 where A_t and A_0 represent the absorbance values at irradiation time t and 0 h, respectively. Data are presented as mean ± SD from three independent experiments.

The photodegradation profiles were further analyzed using a pseudo-first-order kinetic model by plotting $\ln(A_t/A_0)$ against irradiation time (Figure S5). The apparent photodegradation rate constant of quercetin-loaded r-glucan NPs ($0.0930 \pm 0.0029\ h^{-1}$) was significantly lower than those of free quercetin ($0.1597 \pm 0.0133\ h^{-1}$) and the quercetin/β-CD complex ($0.1513 \pm 0.0022\ h^{-1}$), whereas no significant difference was observed between free quercetin and the quercetin/β-CD complex (one-way ANOVA followed by Tukey's HSD test, $p < 0.05$; mean ± SD, $n = 3$). Thus, the photodegradation of quercetin proceeded more slowly in the r-glucan NP system than in the other two systems. This kinetic analysis quantitatively supports the enhanced photostability provided by r-glucan NPs.

The pH-dependent stability of quercetin was then evaluated under strongly acidic and intestinal pH conditions, corresponding to pH 1.2 and 6.8, respectively (Figure 7). At pH 1.2, the residual quercetin fractions changed only gradually during incubation, and the degradation profiles of free quercetin, quercetin-loaded r-glucan NPs, and the quercetin/β-CD complex were broadly similar. Thus, neither carrier system showed a clear protective advantage under the strongly acidic conditions examined. In contrast, more pronounced degradation was observed at pH 6.8. Quercetin-loaded r-glucan NPs retained a larger fraction of quercetin than free quercetin and the quercetin/β-CD complex throughout the incubation period. The quercetin/β-CD complex did not show a clear protective effect relative to free quercetin under this near-neutral condition. These results indicate that the stabilizing effect of r-glucan NPs became more evident under conditions in which quercetin degradation proceeded more rapidly.

The pH-dependent degradation profiles were further analyzed using a pseudo-first-order kinetic model (Figure S6). At pH 1.2, the apparent degradation rate constants were $0.0116 \pm 0.0017\ h^{-1}$ for free quercetin, $0.0165 \pm 0.0041\ h^{-1}$ for quercetin-loaded r-glucan NPs, and $0.0142 \pm 0.0011\ h^{-1}$ for the quercetin/β-CD complex (mean ± SD, $n = 3$). No significant overall difference was detected among the three formulations by one-way ANOVA ($p = 0.150$), and Tukey's HSD test identified no significant pairwise differences. These results indicate that carrier association had little measurable effect on the already slow degradation of quercetin under strongly acidic conditions. Therefore, the present results do not demonstrate a clear protective effect of either r-glucan NPs or β-CD at pH 1.2.

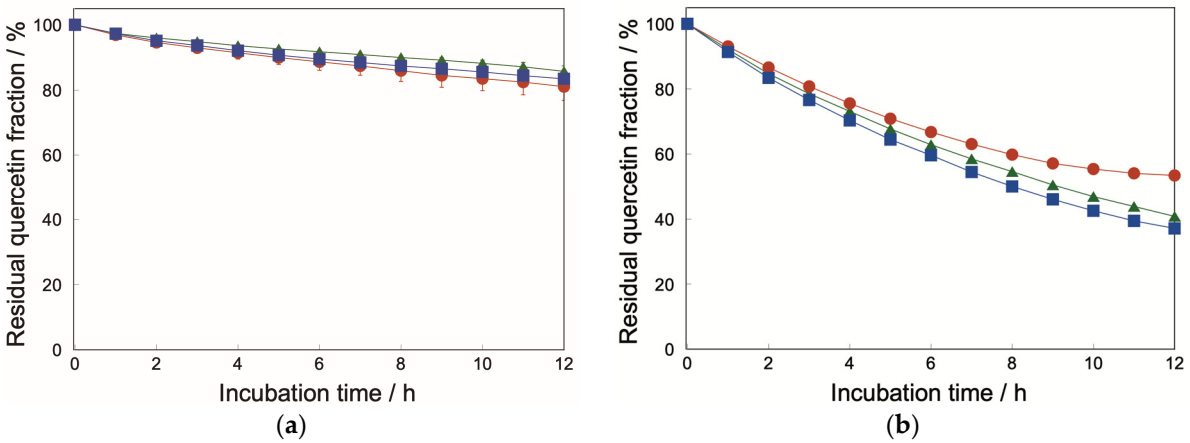

Figure 7. pH-dependent degradation profiles of free and carrier-associated quercetin. Time-dependent changes in the residual quercetin fraction of free quercetin, quercetin-loaded r-glucan NPs, and the quercetin/β-CD complex at (**a**) pH 1.2 and (**b**) pH 6.8 during incubation at 37 °C. The initial quercetin concentration was 25 μM, and the final solvent composition was pH solution/water/ethanol = 89/10/1 (*v*/*v*/*v*). Free quercetin, quercetin-loaded r-glucan NPs, and the quercetin/β-CD complex are shown as green triangles, red circles, and blue squares, respectively. The residual fraction was calculated as A_t/A_0 where A_t and A_0 represent the absorbance values at incubation time t and 0 h, respectively. Data are presented as mean ± SD from three independent experiments.

At pH 6.8, clearer differences among the formulations were observed. The apparent degradation rate constants were 0.0741 ± 0.0010 h^{-1} for free quercetin, 0.0533 ± 0.0004 h^{-1} for quercetin-loaded r-glucan NPs, and 0.0832 ± 0.0027 h^{-1} for the quercetin/β-CD complex (mean ± SD, n = 3). A significant overall difference was detected among the three formulations by one-way ANOVA ($p < 0.05$). Tukey's HSD test showed that the apparent degradation rate constant of quercetin-loaded r-glucan NPs was significantly lower than those of free quercetin and the quercetin/β-CD complex, whereas that of the quercetin/β-CD complex was significantly higher than that of free quercetin ($p < 0.05$). Thus, r-glucan NPs reduced the apparent degradation rate by approximately 28% compared with free quercetin and by approximately 36% compared with the quercetin/β-CD complex. In contrast, the quercetin/β-CD complex showed an approximately 12% higher apparent degradation rate than free quercetin, suggesting that β-CD did not effectively protect quercetin under intestinal pH conditions. The limited protective effect of β-CD at pH 6.8 may also be related to the ionization state of quercetin. The first acid dissociation constant (pK_{a1}) of quercetin has been reported to be approximately 7.2 [35]. Therefore, at pH 6.8, a non-negligible fraction of quercetin molecules may exist as deprotonated phenolate species. Partial deprotonation is expected to increase the polarity and hydration of quercetin and may weaken its affinity for the hydrophobic cavity of β-CD. Consequently, partial deprotonation of quercetin at pH 6.8 may facilitate dissociation from the β-CD cavity, increasing its exposure to the aqueous environment and accelerating degradation. This interpretation is consistent with the observation that the quercetin/β-CD complex did not effectively suppress quercetin degradation under intestinal pH conditions. In contrast, quercetin-loaded r-glucan NPs showed improved stability at pH 6.8. This difference may arise from the polymeric and multivalent nature of the r-glucan NP carrier. The heterogeneous cavity-like microenvironments and multiple interaction sites within the glucan nanoparticles may provide stabilizing interactions that help quercetin remain associated with the carrier even under conditions where partial ionization occurs. Thus, r-glucan NPs may better protect quercetin from pH-induced degradation than β-CD under near-neutral intestinal conditions.

Overall, r-glucan NPs did not provide a clear stability advantage under the strongly acidic pH 1.2 condition, where quercetin degradation was slow for all formulations and no significant difference was observed among their apparent degradation rate constants. By contrast, at pH 6.8, quercetin-loaded r-glucan NPs showed a significantly lower apparent degradation rate constant than both free quercetin and the quercetin/β-CD complex. These findings suggest that r-glucan NPs provide improved protection against quercetin degradation under near-neutral conditions relevant to the intestinal environment.

3.6. Cytotoxicity and Cellular Antioxidant Activity

The preceding cell-free assays demonstrated that r-glucan NPs enhanced the apparent aqueous solubility/dispersibility, formulation-level antioxidant capacity, sustained retention, photostability, and pH-dependent stability of quercetin. To determine whether these physicochemical advantages translated into cellular functionality, we next evaluated the effects of the three quercetin formulations on Caco-2 cell viability and cellular antioxidant activity using Caco-2 cells as an intestinal epithelial model [31].

Before evaluating cellular antioxidant activity, the effects of the three quercetin formulations on Caco-2 cells were examined using an MTT assay. Caco-2 cells were exposed to free quercetin, the quercetin/β-CD complex, or quercetin-loaded r-glucan NPs for 24 h, and cell viability was then evaluated. As shown in Figure 8, cell viability generally decreased with increasing quercetin concentration for all three formulations. No significant differences among the formulations were observed at quercetin concentrations of 7.5, 15, 30, 75, or 100 μM. At 45 μM, cell viability was significantly lower for the quercetin/β-CD complex than for free quercetin and quercetin-loaded r-glucan NPs, whereas no significant difference was observed between free quercetin and quercetin-loaded r-glucan NPs. At 60 μM, cell viability was significantly higher for quercetin-loaded r-glucan NPs than for the quercetin/β-CD complex, whereas free quercetin did not differ significantly from either carrier-associated formulation. Because these significant differences were restricted to 45 and 60 μM and were not consistently observed across the examined concentration range, the overall cell-viability profiles of the three formulations were considered broadly comparable. Thus, loading quercetin into r-glucan NPs did not cause a consistent additional reduction in cell viability relative to the other quercetin formulations under the present experimental conditions. The cellular antioxidant activity results at the higher concentrations were interpreted in conjunction with the relevant cell-viability profiles.

The cellular antioxidant activity of each formulation was then evaluated in Caco-2 cells under AAPH-induced oxidative stress conditions. Caco-2 cells are widely used as an intestinal epithelial cell model and are therefore suitable for evaluating the cellular antioxidant potential of orally relevant bioactive compounds [31,34]. In this assay, intracellular oxidative stress was induced by AAPH-derived peroxyl radicals, and the ability of each quercetin formulation to suppress oxidative stress was compared.

As shown in Figure 9, all three quercetin formulations exhibited concentration-dependent cellular antioxidant activity. Quercetin-loaded r-glucan NPs showed significantly higher CAA values than free quercetin at all examined concentrations from 10 to 50 μM. Compared with the quercetin/β-CD complex, quercetin-loaded r-glucan NPs showed significantly higher CAA values at 10, 20, and 40 μM, whereas no significant differences were observed at 30 and 50 μM. The quercetin/β-CD complex showed significantly higher CAA values than free quercetin at 30, 40, and 50 μM, but not at 10 or 20 μM. This trend differs from the ORAC results obtained at a fixed quercetin concentration in the cell-free system, where free quercetin showed the highest apparent radical-scavenging activity. This discrepancy indicates that cellular antioxidant performance is not governed solely by the intrinsic radical-scavenging activity of quercetin molecules. Instead, aqueous

dispersibility, stability during incubation, cellular availability, and the release or exposure behavior of quercetin from the carrier system likely play important roles.

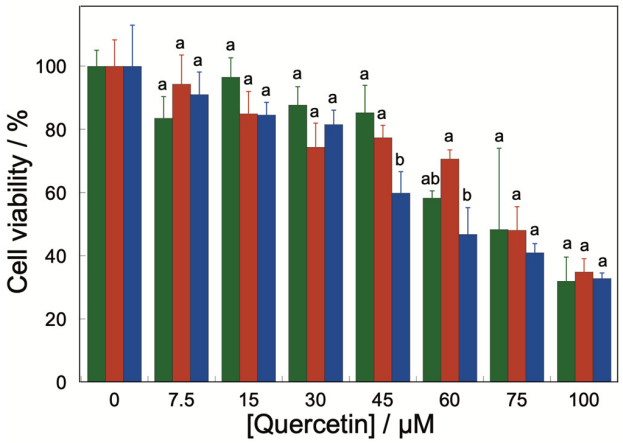

Figure 8. Effects of free and carrier-associated quercetin on Caco-2 cell viability. Caco-2 cells were exposed to free quercetin, quercetin-loaded r-glucan NPs, or the quercetin/β-CD complex at the indicated quercetin concentrations for 24 h at 37 °C under 5% CO_2. Cell viability was evaluated using the MTT assay. Values for free quercetin were expressed relative to the 0.1% DMSO vehicle control, whereas values for the aqueous r-glucan NP and β-CD formulations were expressed relative to the corresponding untreated control. Free quercetin, quercetin-loaded r-glucan NPs, and the quercetin/β-CD complex are shown in green, red, and blue, respectively. Data are presented as mean ± SD from three independent experiments. At each quercetin concentration, differences among the three formulations were analyzed by one-way ANOVA followed by Tukey's HSD multiple-comparison test. Different lowercase letters indicate significant differences among the formulations at the same quercetin concentration ($p < 0.05$); groups sharing at least one letter are not significantly different.

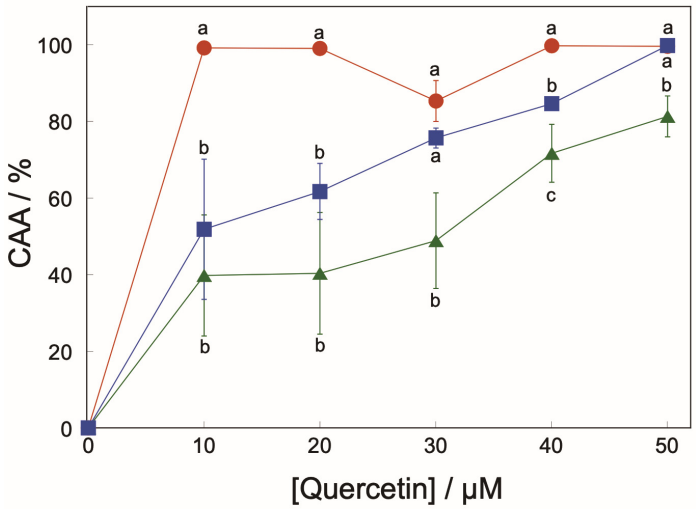

Figure 9. Cellular antioxidant activity of free and carrier-associated quercetin in Caco-2 cells. Cellular antioxidant activity (CAA) was evaluated after exposing Caco-2 cells to free quercetin, quercetin-loaded r-glucan NPs, or the quercetin/β-CD complex at the indicated quercetin concentrations, followed by induction of oxidative stress with 500 μM AAPH. Free quercetin, quercetin-loaded r-glucan NPs, and the quercetin/β-CD complex are shown in green, red, and blue, respectively. CAA values were calculated from the fluorescence intensity–time curves relative to the AAPH-treated control and the no-AAPH blank. Data are presented as mean ± SD from three independent experiments. At each quercetin concentration, differences among the three formulations were analyzed by one-way ANOVA followed by Tukey's HSD multiple-comparison test. Different lowercase letters indicate significant differences among the formulations at the same quercetin concentration ($p < 0.05$); groups sharing at least one letter are not significantly different.

Free quercetin is highly active when molecularly available, but its poor aqueous solubility and tendency to precipitate or aggregate can limit the amount of quercetin that remains accessible to cells. Similarly, although β-CD improved the apparent aqueous solubility/dispersibility of quercetin, partial inclusion, secondary aggregation, and limited protection under near-neutral pH conditions may restrict the effective availability of quercetin in the cellular environment. In contrast, r-glucan NPs maintained quercetin in a water-dispersible and carrier-associated state while providing protection against pH-dependent degradation. As shown in the preceding sections, r-glucan NPs enhanced aqueous dispersibility, preserved a substantial fraction of antioxidant activity, slowed the apparent loss of carrier-associated quercetin, and improved quercetin stability under gastrointestinal pH conditions. These combined properties likely contributed to the higher cellular antioxidant activity observed for quercetin-loaded r-glucan NPs.

The significantly higher CAA values of quercetin-loaded r-glucan NPs at relatively low quercetin concentrations suggest that this carrier maintained quercetin in a cellularly effective antioxidant form. Overall, the physicochemical advantages of r-glucan NPs translated into enhanced antioxidant performance in the Caco-2 model.

3.7. Oxidative-Stress-Responsive Behavior

To explore whether the glucan carrier could undergo structural changes under radical-generating conditions, we examined the effect of AAPH-derived peroxyl radicals on the molecular weight of the glucan chains constituting r-glucan NPs.

The molecular-weight distribution of glucan chains after incubation with AAPH was analyzed by GPC (Figure 10). With increasing incubation time, the molecular-weight distribution shifted toward the lower-molecular-weight region. In addition, the weight-average molecular weight (M_w) decreased over time. These results indicate that AAPH-generated peroxyl radicals cleaved the β-1,3-1,6-glucan chains constituting r-glucan NPs under the present oxidative conditions.

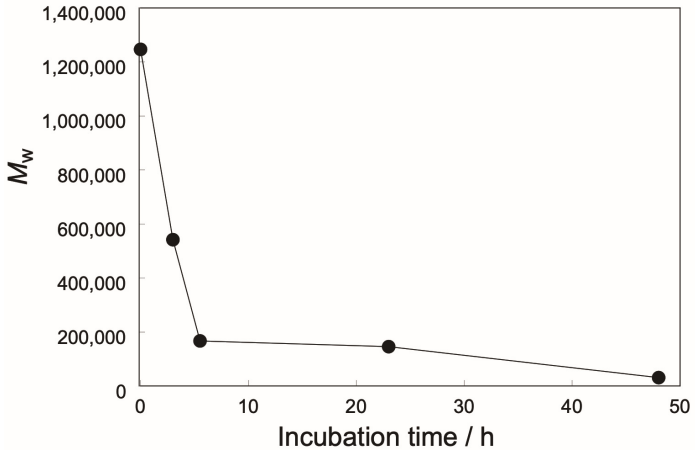

Figure 10. AAPH-induced decrease in the molecular weight of glucan chains constituting r-glucan NPs. r-Glucan NPs were incubated with AAPH at final concentrations of 20 mM glucan, on a glucose-unit basis, and 20 mM AAPH at 37 °C. Samples were collected at 0, 3, 5.5, 23, and 48 h, and the molecular-weight distributions of the constituent glucan chains were analyzed by gel permeation chromatography (GPC). The weight-average molecular weight (M_w) is plotted as a function of incubation time.

This oxidative degradation could alter the hydrophobic, cavity-rich microenvironments that retain quercetin and thereby increase the accessibility or release of carrier-associated quercetin. This interpretation is consistent with our previous finding that lower-molecular-weight glucan chains formed less developed cavity structures and re-

leased incorporated curcumin rapidly than higher-molecular-weight glucan chains [22]. Therefore, the AAPH-induced decrease in glucan molecular weight may facilitate the quercetin release or exposure under radical-generating conditions.

These findings provide a possible mechanistic context for the difference between the cell-free ORAC and CAA results. Although quercetin-loaded r-glucan NPs showed lower ORAC activity than free quercetin at an equal quercetin concentration, partial degradation of the glucan chains under radical-generating conditions could increase the accessibility of carrier-associated quercetin.

It should be noted that the present GPC experiment demonstrates oxidative degradation of the glucan carrier but does not directly quantify quercetin release in the presence of AAPH. Therefore, the oxidative-stress-responsive release mechanism should be regarded as a plausible interpretation rather than direct proof. Nevertheless, the combination of enhanced cellular antioxidant activity and AAPH-induced glucan chain degradation supports the possibility that r-glucan NPs are not simply passive solubilizing carriers. Rather, they may function as a food-compatible antioxidant delivery system that combines high aqueous dispersibility, sustained retention under normal conditions, protective stabilization, and oxidative-stress-responsive exposure or release of quercetin.

4. Conclusions

In this study, alkali-neutralization-induced β-1,3-1,6-glucan nanoparticles (r-glucan NPs) were evaluated as a food-compatible carrier for quercetin. Compared with β-CD, r-glucan NPs showed higher quercetin loading, greater apparent aqueous solubility/dispersibility, slower apparent loss of carrier-associated quercetin, and improved photostability and reduced quercetin degradation at pH 6.8. Spectroscopic analyses were consistent with quercetin association within chiral, cavity-rich glucan microenvironments. Native t-glucan initially retained quercetin but failed to maintain a homogeneous dispersion in 1 vol% ethanol, indicating that alkali-neutralization-induced glucan reassembly was important for sustained aqueous dispersion. Although carrier association reduced ORAC activity at an equal quercetin concentration, the high aqueous loading of r-glucan NPs enabled a substantially greater maximum antioxidant capacity under the present assay conditions. Quercetin-loaded r-glucan NPs also showed a broadly comparable cell-viability profile and higher cellular antioxidant activity than free quercetin, with advantages over β-CD at selected concentrations. AAPH-induced decreases in glucan molecular weight suggest possible oxidative-stress-responsive behavior, although direct quercetin release remains to be demonstrated.

Supplementary Materials: The following supporting information can be downloaded at: https://www.mdpi.com/article/10.3390/nutraceuticals6030053/s1. Figure S1: Dispersion behavior of blank and quercetin-treated t-glucan. (a) Representative number-weighted hydrodynamic size distributions of blank t-glucan (blue), quercetin-treated t-glucan in water (red), and quercetin-treated t-glucan containing 1 vol% ethanol immediately after ethanol addition (green), measured by dynamic light scattering at 25 °C. (b) Representative photograph of the quercetin-treated t-glucan sample immediately after ethanol addition to a final concentration of 1 vol%. (c) Representative photograph of the same sample after storage for 3 days at 25 °C under light-protected conditions, showing increased turbidity and visible precipitation; Figure S2: Number-weighted hydrodynamic size distributions of blank r-glucan NPs, quercetin-loaded r-glucan NPs, and the quercetin/β-CD complex measured by dynamic light scattering. Blank r-glucan NPs, quercetin-loaded r-glucan NPs, and the quercetin/β-CD complex are shown in green, red, and blue, respectively. Measurements were performed at 25 °C using the supernatants obtained after centrifugation; Figure S3: Representative photographs of saturated aqueous supernatants of free quercetin, quercetin-loaded r-glucan NPs, and the quercetin/β-CD complex. Photographs show the supernatants obtained after centrifugation

of saturated aqueous solutions/dispersions of (a) free quercetin, (b) quercetin-loaded r-glucan NPs, and (c) the quercetin/β-CD complex. The more intense yellow color of the r-glucan NP sample indicates that a larger amount of quercetin was retained in the aqueous phase; Figure S4: Apparent pseudo-first-order analysis of the loss of carrier-associated quercetin from quercetin-loaded r-glucan NPs and the quercetin/β-CD complex. The residual fraction of carrier-associated quercetin was analyzed by plotting $\ln(A_t/A_0)$ against incubation time. Quercetin-loaded r-glucan NPs and the quercetin/β-CD complex are shown as red circles and blue squares, respectively. Solid lines indicate linear least-squares fits. A_t and A_0 represent the absorbance values of quercetin at time t and 0 h, respectively; Figure S5: Apparent pseudo-first-order analysis of quercetin photodegradation under fluorescent light irradiation. The residual quercetin fraction was analyzed by plotting $\ln(A_t/A_0)$ against irradiation time. Free quercetin, quercetin-loaded r-glucan NPs, and the quercetin/β-CD complex are shown as green triangles, red circles, and blue squares, respectively. Solid lines indicate linear least-squares fits. A_t and A_0 represent the absorbance values of quercetin at time t and 0 h, respectively; Figure S6: Apparent pseudo-first-order analysis of pH-dependent quercetin degradation at (a) pH 1.2 and (b) pH 6.8. The residual quercetin fraction was analyzed by plotting $\ln(A_t/A_0)$ against incubation time. Free quercetin, quercetin-loaded r-glucan NPs, and the quercetin/β-CD complex are shown as green triangles, red circles, and blue squares, respectively. Solid lines indicate linear least-squares fits. A_t and A_0 represent the absorbance values of quercetin at time t and 0 h, respectively.

Author Contributions: Conceptualization, K.K.; methodology, K.K.; validation, S.K. and N.D.; formal analysis, S.K.; investigation, S.K. and N.D.; resources, T.S.; data curation, S.K.; writing—original draft preparation, K.K. and T.S.; writing—review and editing, K.K. and T.S.; supervision, K.K.; project administration, K.K.; funding acquisition, K.K. All authors have read and agreed to the published version of the manuscript.

Funding: This work was supported by the Hirao Taro Foundation of Konan Gakuen for Academic Research, Japan.

Institutional Review Board Statement: Not applicable.

Informed Consent Statement: Not applicable.

Data Availability Statement: The data supporting the findings of this study are included in this article and its Supplementary Materials. Additional data are available from the corresponding author upon reasonable request.

Conflicts of Interest: Kazuya Koumoto is a professor at Konan University and the CEO of B-Lab Co., Ltd., which is involved in the development and commercialization of β-glucan-based nanomaterials related to the materials described in this study. This relationship may be perceived as a potential conflict of interest. The study was conducted as part of a master's thesis research project at Konan University. B-Lab Co., Ltd. and the funder had no role in the design of the study; in the collection, analyses, or interpretation of data; in the writing of the manuscript; or in the decision to publish the results. The remaining authors declare no conflicts of interest.

Abbreviations

The following abbreviations are used in this manuscript:

AAPH	2,2′-azobis(2-amidinopropane) dihydrochloride
AUC	area under the curve
β-CD	β-cyclodextrin
CAA	cellular antioxidant activity
CD	circular dichroism
DCFH-DA	2′,7′-dichlorodihydrofluorescein diacetate
DLS	dynamic light scattering
DMEM	Dulbecco's modified Eagle's medium
FBS	fetal bovine serum

GPC	gel permeation chromatography
ICD	induced circular dichroism
MTT	3-(4,5-Dimethyl-2-thiazolyl)-2,5-diphenyl-2H-tetrazolium bromide
M_n	number-average molecular weight
M_w	weight-average molecular weight
ORAC	oxygen radical absorbance capacity
PBS	phosphate-buffered saline
PDI	polydispersity index
r-glucan NPs	renatured β-1,3-1,6-glucan nanoparticles

References

1. Aghababaei, F.; Hadidi, M. Recent Advances in Potential Health Benefits of Quercetin. *Pharmaceuticals* **2023**, *16*, 1020. [CrossRef] [PubMed]
2. Frenț, O.-D.; Ștefan, L.; Morgovan, C.M.; Duțeanu, N.; Dejeu, I.L.; Marian, E.; Vicaș, L.; Manole, F. A Systematic Review: Quercetin—Secondary Metabolite of the Flavonol Class, with Multiple Health Benefits and Low Bioavailability. *Int. J. Mol. Sci.* **2024**, *25*, 12091. [CrossRef] [PubMed]
3. Manta, K.; Papakyriakopoulou, P.; Chountoulesi, M.; Diamantis, D.A.; Spaneas, D.; Vakali, V.; Naziris, N.; Chatziathanasiadou, M.V.; Andreadelis, I.; Moschovou, K.; et al. Preparation and Biophysical Characterization of Quercetin Inclusion Complexes with β-Cyclodextrin Derivatives to Be Formulated as Possible Nose-to-Brain Quercetin Delivery Systems. *Mol. Pharm.* **2020**, *17*, 4241–4255. [CrossRef] [PubMed]
4. Wang, H.; Di, W.; Gao, X.; Guo, Y.; Tang, T.; Bai, X.; Cao, H. Materials, Syntheses and Biomedical Applications of Nano-Quercetin Formulations. *Int. J. Nanomed.* **2025**, *20*, 8729–8764. [CrossRef] [PubMed]
5. Bai, C.; Hu, X.; Lu, S.; Xu, B.; Ma, T.; Song, Y. Recent Advances and Application Challenges of Quercetin-Loaded Delivery Systems: From Material Selection to Bioavailability. *J. Future Foods* **2025**, *in press*. [CrossRef]
6. Osojnik Črnivec, I.G.; Skrt, M.; Polak, T.; Šeremet, D.; Mrak, P.; Komes, D.; Vrhovšek, U.; Poklar Ulrih, N. Aspects of Quercetin Stability and Its Liposomal Enhancement in Yellow Onion Skin Extracts. *Food Chem.* **2024**, *459*, 140347. [CrossRef] [PubMed]
7. Liu, S.; Han, Y.; Liu, X.; Wang, R.; Sun, B.; Nakabayashi, A.; Chai, J.; Li, D. Improving the Solubilization, Stability, Dialysis Performance and Antioxidant Properties of Quercetin in Surfactant-Free Microemulsion. *J. Mol. Liq.* **2024**, *409*, 125531. [CrossRef]
8. Kim, E.S.; Kim, D.Y.; Lee, J.-S.; Lee, H.G. Quercetin Delivery Characteristics of Chitosan Nanoparticles Prepared with Different Molecular Weight Polyanion Cross-Linkers. *Carbohydr. Polym.* **2021**, *267*, 118157. [CrossRef] [PubMed]
9. Liao, L.; McClements, D.J.; Chen, X.; Zhu, Y.; Liu, Y.; Liang, R.; Zou, L.; Liu, W. Dietary proteins as excipient ingredients for improving the solubility, stability, and bioaccessibility of quercetin: Role of intermolecular interactions. *Food Res. Int.* **2022**, *161*, 111806. [CrossRef] [PubMed]
10. Nagaraj, K.; Karuppiah, C.; Wadaan, M.A.; Maity, P.; Kaliyaperumal, R.; Vaishnavi, E.; Rajaraman, D.; Abhijith, S.M.; Ramaraj, S.K.; Mathivanan, I. Synthesis, Characterization, Molecular Modeling, Binding Energies of β-Cyclodextrin-Inclusion Complexes of Quercetin: Modification of Photo Physical Behavior upon β-CD Complexation. *Spectrochim. Acta A Mol. Biomol. Spectrosc.* **2024**, *313*, 124091. [CrossRef] [PubMed]
11. Azzi, J.; Jraij, A.; Auezova, L.; Fourmentin, S.; Greige-Gerges, H. Novel Findings for Quercetin Encapsulation and Preservation with Cyclodextrins, Liposomes, and Drug-in-Cyclodextrin-in-Liposomes. *Food Hydrocoll.* **2018**, *81*, 328–340. [CrossRef]
12. Chen, X.; Chen, Y.; Huang, Y.; Zou, L.; Liu, C.; McClements, D.J.; Liu, W. Hybrid bionanoparticle-stabilized Pickering emulsions for quercetin delivery: Effect of interfacial composition on release, lipolysis, and bioaccessibility. *ACS Appl. Nano Mater.* **2019**, *2*, 6462–6472. [CrossRef]
13. Moon, H.; Lertpatipanpong, P.; Hong, Y.; Kim, C.T.; Baek, S.J. Nano-Encapsulated Quercetin by Soluble Soybean Polysaccharide/Chitosan Enhances Anti-Cancer, Anti-Inflammation, and Anti-Oxidant Activities. *J. Funct. Foods* **2021**, *87*, 104756. [CrossRef]
14. Aluani, D.; Tzankova, V.; Kondeva-Burdina, M.; Yordanov, Y.; Nikolova, E.; Odzhakov, F.; Apostolov, A.; Markova, T.; Yoncheva, K. Evaluation of biocompatibility and antioxidant efficiency of chitosan-alginate nanoparticles loaded with quercetin. *Int. J. Biol. Macromol.* **2017**, *103*, 771–782. [CrossRef] [PubMed]
15. Jiang, F.; Du, C.; Zhao, N.; Jiang, W.; Yu, X.; Du, S. Preparation and characterization of quinoa starch nanoparticles as quercetin carriers. *Food Chem.* **2022**, *369*, 130895. [CrossRef] [PubMed]
16. Davoudi, Z.; Azizi, M.H.; Barzegar, M.; Bernkop-Schnürch, A. Porous starch-inulin loaded quercetin microcapsules: Characterization, antioxidant activity, in-vitro release, and storage stability. *J. Pharm. Sci.* **2024**, *113*, 1228–1238. [CrossRef] [PubMed]
17. Mochizuki, S.; Sakurai, K. A Novel Polysaccharide/Polynucleotide Complex and Its Application to Bio-Functional DNA Delivery System. *Polym. J.* **2009**, *41*, 343–353. [CrossRef]

18. Suzuki, T.; Kusano, K.; Kondo, N.; Nishikawa, K.; Nakano, M.; Ohno, N. Biological Activity of High-Purity β-1,3-1,6-Glucan Derived from *Aureobasidium pullulans*: A Literature Review. *Nutrients* **2021**, *13*, 242. [CrossRef] [PubMed]
19. Kodama, A.; Nakagawa, A.; Nonoguchi, Y.; Sakurai, H.; Yano, C.; Suzuki, T.; Koumoto, K. Solubilization of Poorly Water-Soluble Bioactive Molecules in Neutral Aqueous Media by Complexation with Renatured β-1,3-1,6-Glucan Nanoparticles. *Biopolymers* **2020**, *111*, e23349. [CrossRef] [PubMed]
20. Ruphuy, G.; Saloň, I.; Tomas, J.; Šalamúnová, P.; Hanuš, J.; Štěpánek, F. Encapsulation of Poorly Soluble Drugs in Yeast Glucan Particles by Spray Drying Improves Dispersion and Dissolution Properties. *Int. J. Pharm.* **2020**, *576*, 118990. [CrossRef] [PubMed]
21. Šalamúnová, P.; Saloň, I.; Ruphuy, G.; Kroupová, J.; Balouch, M.; Hanuš, J.; Štěpánek, F. Evaluation of β-Glucan Particles as Dual-Function Carriers for Poorly Soluble Drugs. *Eur. J. Pharm. Biopharm.* **2021**, *168*, 15–25. [CrossRef] [PubMed]
22. Nonoguchi, Y.; Kodama, A.; Unesaki, R.; Doi, N.; Suzuki, T.; Koumoto, K. Modification of the Release Rate of Curcumin from the Cavity of Renatured β-1,3-1,6-Glucan Nanoparticles by Changing the Molecular Weight of the Constituent Polysaccharide Chains. *Chem. Lett.* **2020**, *49*, 1150–1153. [CrossRef]
23. Dall'Acqua, S.; Miolo, G.; Innocenti, G.; Caffieri, S. The Photodegradation of Quercetin: Relation to Oxidation. *Molecules* **2012**, *17*, 8898–8907. [CrossRef] [PubMed]
24. Jurasekova, Z.; Domingo, C.; García-Ramos, J.V.; Sánchez-Cortés, S. Effect of pH on the Chemical Modification of Quercetin and Structurally Related Flavonoids Characterized by Optical (UV-Visible and Raman) Spectroscopy. *Phys. Chem. Chem. Phys.* **2014**, *16*, 12802–12811. [CrossRef] [PubMed]
25. Kellil, A.; Grigorakis, S.; Loupassaki, S.; Makris, D.P. Empirical Kinetic Modelling and Mechanisms of Quercetin Thermal Degradation in Aqueous Model Systems: Effect of pH and Addition of Antioxidants. *Appl. Sci.* **2021**, *11*, 2579. [CrossRef]
26. Dubois, M.; Gilles, K.A.; Hamilton, J.K.; Rebers, P.A.; Smith, F. Colorimetric Method for Determination of Sugars and Related Substances. *Anal. Chem.* **1956**, *28*, 350–356. [CrossRef]
27. Zornoza, A.; Vélaz, I.; González-Gaitano, G.; Martínez-Oharriz, M.C. A Comprehensive Study of Gemfibrozil Complexation with β-Cyclodextrins in Aqueous Solution Using Different Analytical Techniques. *Int. J. Mol. Sci.* **2022**, *23*, 16119. [CrossRef] [PubMed]
28. Koontz, J.L.; Marcy, J.E.; O'Keefe, S.F.; Duncan, S.E. Cyclodextrin Inclusion Complex Formation and Solid-State Characterization of the Natural Antioxidants α-Tocopherol and Quercetin. *J. Agric. Food Chem.* **2009**, *57*, 1162–1171. [CrossRef] [PubMed]
29. Li, X.; Liu, Y.; Zheng, J.; Zhu, X.; Fang, W.; Lei, S.; Zhuang, W.; Wu, J.; Hao, T.; You, S.; et al. β-Cyclodextrin/Thymol Microcapsule-Embedded Starch Coatings for Synchronized Antimicrobial Release and Shelf-Life Extension in Blueberries. *Foods* **2025**, *14*, 3132. [CrossRef] [PubMed]
30. Watanabe, J.; Oki, T.; Takebayashi, J.; Yamasaki, K.; Takano-Ishikawa, Y.; Hino, A.; Yasui, A. Method Validation by Interlaboratory Studies of Improved Hydrophilic Oxygen Radical Absorbance Capacity Methods for the Determination of Antioxidant Capacities of Antioxidant Solutions and Food Extracts. *Anal. Sci.* **2012**, *28*, 159–165. [CrossRef] [PubMed]
31. Sambuy, Y.; De Angelis, I.; Ranaldi, G.; Scarino, M.L.; Stammati, A.; Zucco, F. The Caco-2 Cell Line as a Model of the Intestinal Barrier: Influence of Cell and Culture-Related Factors on Caco-2 Cell Functional Characteristics. *Cell Biol. Toxicol.* **2005**, *21*, 1–26. [CrossRef] [PubMed]
32. Mosmann, T. Rapid Colorimetric Assay for Cellular Growth and Survival: Application to Proliferation and Cytotoxicity Assays. *J. Immunol. Methods* **1983**, *65*, 55–63. [CrossRef] [PubMed]
33. Wolfe, K.L.; Liu, R.H. Cellular Antioxidant Activity (CAA) Assay for Assessing Antioxidants, Foods, and Dietary Supplements. *J. Agric. Food Chem.* **2007**, *55*, 8896–8907. [CrossRef] [PubMed]
34. Kellett, M.E.; Greenspan, P.; Pegg, R.B. Modification of the Cellular Antioxidant Activity (CAA) Assay to Study Phenolic Antioxidants in a Caco-2 Cell Line. *Food Chem.* **2018**, *244*, 359–363. [CrossRef] [PubMed]
35. Herrero-Martínez, J.M.; Sanmartin, M.; Rosés, M.; Bosch, E.; Ràfols, C. Determination of Dissociation Constants of Flavonoids by Capillary Electrophoresis. *Electrophoresis* **2005**, *26*, 1886–1895. [CrossRef] [PubMed]